

ISSN 2523-6806

Volume 7, Issue 19 — January — June - 2023



Journal of
Technological
Operations

ECORFAN[®]

ECORFAN-Taiwan

Chief Editor

BARRERO-ROSALES, José Luis. PhD

Executive Director

RAMOS-ESCAMILLA, María. PhD

Editorial Director

PERALTA-CASTRO, Enrique. MsC

Web Designer

ESCAMILLA-BOUCHAN, Imelda. PhD

Web Diagrammer

LUNA-SOTO, Vladimir. PhD

Editorial Assistant

SORIANO-VELASCO, Jesús. BsC

Philologist

RAMOS-ARANCIBIA, Alejandra. BsC

Journal of Technological Operations,
Volume 7, Issue 19, January - June 2023,
is a journal edited semestral by
ECORFAN. Taiwan, Taipei. YongHe
district, Zhong Xin, Street 69. Postcode:
23445. WEB:

www.ecorfan.org/taiwan/journal@ecorfan.org. Editor in Chief: BARRERO-ROSALES, José Luis. PhD. ISSN: 2523-6806. Responsible for the latest update of this number ECORFAN Computer Unit. ESCAMILLA-BOUCHÁN, Imelda. PhD, LUNA-SOTO, Vladimir. PhD, last updated June 30, 2023.

The opinions expressed by the authors do not necessarily reflect the views of the editor of the publication.

It is strictly forbidden to reproduce any part of the contents and images of the publication without permission of the National Institute for the Defense of Competition and Protection of Intellectual Property.

Journal of Technological Operations

Definition of Research Journal

Scientific Objectives

Support the international scientific community in its written production Science, Technology and Innovation in the Field of Engineering and Technology, in Subdisciplines production systems, mechanical properties, data transmission, process standardization, industrial engineering, composite materials, kinematic analysis, kinetic study, power generator, industrial and technological processes..

ECORFAN-Mexico SC is a Scientific and Technological Company in contribution to the Human Resource training focused on the continuity in the critical analysis of International Research and is attached to CONAHCYT-RENIICYT number 1702902, its commitment is to disseminate research and contributions of the International Scientific Community, academic institutions, agencies and entities of the public and private sectors and contribute to the linking of researchers who carry out scientific activities, technological developments and training of specialized human resources with governments, companies and social organizations.

Encourage the interlocution of the International Scientific Community with other Study Centers in Mexico and abroad and promote a wide incorporation of academics, specialists and researchers to the publication in Science Structures of Autonomous Universities - State Public Universities - Federal IES - Polytechnic Universities - Technological Universities - Federal Technological Institutes - Normal Schools - Decentralized Technological Institutes - Intercultural Universities - S & T Councils - CONAHCYT Research Centers.

Scope, Coverage and Audience

Journal of Technological Operations is a Research Journal edited by ECORFAN-Mexico S.C in its Holding with repository in Taiwan, is a scientific publication arbitrated and indexed with semester periods. It supports a wide range of contents that are evaluated by academic peers by the Double-Blind method, around subjects related to the theory and practice of production systems, mechanical properties, data transmission, process standardization, industrial engineering, composite materials, kinematic analysis, kinetic study, power generator, industrial and technological processes with diverse approaches and perspectives, That contribute to the diffusion of the development of Science Technology and Innovation that allow the arguments related to the decision making and influence in the formulation of international policies in the Field of Engineering and Technology. The editorial horizon of ECORFAN-Mexico® extends beyond the academy and integrates other segments of research and analysis outside the scope, as long as they meet the requirements of rigorous argumentative and scientific, as well as addressing issues of general and current interest of the International Scientific Society.

Editorial Board

MAYORGA - ORTIZ, Pedro. PhD
Institut National Polytechnique de Grenoble

DECTOR - ESPINOZA, Andrés. PhD
Centro de Microelectrónica de Barcelona

CASTILLO - LÓPEZ, Oscar. PhD
Academia de Ciencias de Polonia

HERNANDEZ - ESCOBEDO, Quetzalcoatl Cruz. PhD
Universidad Central del Ecuador

FERNANDEZ - ZAYAS, José Luis. PhD
University of Bristol

HERRERA - DIAZ, Israel Enrique. PhD
Center of Research in Mathematics

NAZARIO - BAUTISTA, Elivar. PhD
Centro de Investigacion en óptica y nanofisica

CERCADO - QUEZADA, Bibiana. PhD
Intitut National Polytechnique Toulouse

CARBAJAL - DE LA TORRE, Georgina. PhD
Université des Sciencies et Technologies de Lille

AYALA - GARCÍA, Ivo Neftalí. PhD
University of Southampton

Arbitration Committee

CRUZ - BARRAGÁN, Aidee. PhD
Universidad de la Sierra Sur

CASTILLO - TOPETE, Víctor Hugo. PhD
Centro de Investigación Científica y de Educación Superior de Ensenada

GONZÁLEZ - LÓPEZ, Samuel. PhD
Instituto Nacional de Astrofísica, Óptica y Electrónica

CASTAÑÓN - PUGA, Manuel. PhD
Universidad Autónoma de Baja California

ARROYO - FIGUEROA, Gabriela. PhD
Universidad de Guadalajara

GONZÁLEZ - REYNA, Sheila Esmeralda. PhD
Instituto Tecnológico Superior de Irapuato

BARRON, Juan. PhD
Universidad Tecnológica de Jalisco

ARREDONDO - SOTO, Karina Cecilia. PhD
Instituto Tecnológico de Ciudad Juárez

BAEZA - SERRATO, Roberto. PhD
Universidad de Guanajuato

BAUTISTA - SANTOS, Horacio. PhD
Universidad Popular Autónoma del Estado de Puebla

Assignment of Rights

The sending of an Article to Journal of Technological Operations emanates the commitment of the author not to submit it simultaneously to the consideration of other series publications for it must complement the Originality Format for its Article.

The authors sign the Authorization Format for their Article to be disseminated by means that ECORFAN-Mexico, S.C. In its Holding Taiwan considers pertinent for disclosure and diffusion of its Article its Rights of Work.

Declaration of Authorship

Indicate the Name of Author and Coauthors at most in the participation of the Article and indicate in extensive the Institutional Affiliation indicating the Department.

Identify the Name of Author and Coauthors at most with the CVU Scholarship Number-PNPC or SNI-CONAHCYT- Indicating the Researcher Level and their Google Scholar Profile to verify their Citation Level and H index.

Identify the Name of Author and Coauthors at most in the Science and Technology Profiles widely accepted by the International Scientific Community ORC ID - Researcher ID Thomson - arXiv Author ID - PubMed Author ID - Open ID respectively.

Indicate the contact for correspondence to the Author (Mail and Telephone) and indicate the Researcher who contributes as the first Author of the Article.

Plagiarism Detection

All Articles will be tested by plagiarism software PLAGSCAN if a plagiarism level is detected Positive will not be sent to arbitration and will be rescinded of the reception of the Article notifying the Authors responsible, claiming that academic plagiarism is criminalized in the Penal Code.

Arbitration Process

All Articles will be evaluated by academic peers by the Double Blind method, the Arbitration Approval is a requirement for the Editorial Board to make a final decision that will be final in all cases. MARVID® is a derivative brand of ECORFAN® specialized in providing the expert evaluators all of them with Doctorate degree and distinction of International Researchers in the respective Councils of Science and Technology the counterpart of CONAHCYT for the chapters of America-Europe-Asia- Africa and Oceania. The identification of the authorship should only appear on a first removable page, in order to ensure that the Arbitration process is anonymous and covers the following stages: Identification of the Research Journal with its author occupation rate - Identification of Authors and Coauthors - Detection of plagiarism PLAGSCAN - Review of Formats of Authorization and Originality-Allocation to the Editorial Board- Allocation of the pair of Expert Arbitrators-Notification of Arbitration -Declaration of observations to the Author-Verification of Article Modified for Editing-Publication.

Instructions for Scientific, Technological and Innovation Publication

Knowledge Area

The works must be unpublished and refer to topics of production systems, mechanical properties, data transmission, process standardization, industrial engineering, composite materials, kinematic analysis, kinetic study, power generator, industrial and technological processes and other topics related to Engineering and Technology.

Presentation of the content

In the first article we present, *Precision analysis of the integration rules used for transient simulation in electric networks* by GALVÁN-SÁNCHEZ, Verónica Adriana, BAÑUELOS-CABRAL, Eduardo Salvador, GARCÍA-SÁNCHEZ, Jorge Luis and SOTELO-CASTAÑÓN, Julián, with adscription in the Universidad de Guadalajara, in the next article we present, Maintenance management of pneumatic equipment and facilities at a plant in the Industrial corridor in the South area of the state of Tamaulipas by CRUZ-SUSTAITA, Vianey, LERMA-LEDEZMA, David and ESPINOSA-SOSA, Enrique Esteban, with adscription in the Universidad Politécnica de Altamira, in the next article we present, *Simulation of the behavior of the flow of electrons between the electrodes of a thermionic converter* by CALVARIO-GONZÁLEZ, Abdías, BARBOSA-SANTILLÁN, Luis Francisco and JUÁREZ-VARELA, Mirna Patricia, with adscription in the Universidad Tecnológica de Puebla, in the next article we present, *Integrative project: CNC technology and micro-wire (MIG) welding for precision and efficiency in industry* by ZUNIGA-MORENO, Juan, COTERO-RODRÍGUEZ, Arely Eunice and MORALES HERNÁNDEZ, Victor, with adscription in the Universidad Tecnológica Cadereyta.

Content

Article	Page
Precision analysis of the integration rules used for transient simulation in electric networks GALVÁN-SÁNCHEZ, Verónica Adriana, BAÑUELOS-CABRAL, Eduardo Salvador, GARCÍA-SÁNCHEZ, Jorge Luis and SOTELO-CASTAÑÓN, Julián <i>Universidad de Guadalajara</i>	1-11
Maintenance management of pneumatic equipment and facilities at a plant in the Industrial corridor in the South area of the state of Tamaulipas CRUZ-SUSTAITA, Vianey, LERMA-LEDEZMA, David and ESPINOSA-SOSA, Enrique Esteban <i>Universidad Politécnica de Altamira</i>	12-15
Simulation of the behavior of the flow of electrons between the electrodes of a thermionic converter CALVARIO-GONZÁLEZ, Abdías, BARBOSA-SANTILLÁN, Luis Francisco and JUÁREZ-VARELA, Mirna Patricia <i>Universidad Tecnológica de Puebla</i>	16-30
Integrative project: CNC technology and micro-wire (MIG) welding for precision and efficiency in industry ZUNIGA-MORENO, Juan, COTERO-RODRÍGUEZ, Arely Eunice and MORALES HERNÁNDEZ, Victor <i>Universidad Tecnológica Cadereyta</i>	31-36

Precision analysis of the integration rules used for transient simulation in electric networks

Análisis de la precisión de las reglas de integración utilizadas en la simulación de transitorios eléctricos

GALVÁN-SÁNCHEZ, Verónica Adriana†*, BAÑUELOS-CABRAL, Eduardo Salvador, GARCÍA-SÁNCHEZ, Jorge Luis and SOTELO-CASTAÑÓN, Julián

Universidad de Guadalajara, Departamento de Ingeniería Mecánica Eléctrica del Centro Universitario de Ciencias Exactas e Ingenierías

ID 1st Author: *Verónica Adriana, Galván-Sánchez* / ORC ID: 0000-0002-5462-2361

ID 1st Co-author: *Eduardo Salvador, Bañuelos-Cabral* / ORC ID: 0000-0002-6004-5898

ID 2nd Co-author: *Jorge Luis, García-Sánchez* / ORC ID: 0000-0003-2919-186X

ID 3rd Co-author: *Julián, Sotelo-Castañón* / ORC ID: 0000-0002-9776-5303

DOI: 10.35429/JTO.2023.7.19.1.11

Received March 10, 2023, Accepted, June 30, 2023

Abstract

The adequate selection of the integration rule and time step is crucial to ensure accurate results in the simulation of an electric network. For this reason, this work has two main objectives: to analyze the distortion of the waves due to the integration rule and integration time step, and to provide guidelines for new circuit simulators' users on how to properly choose an integration rule and a time step according to a desired precision. When discretizing a continuous system, the frequency response of the discrete system can be used to evaluate the precision of the mentioned rule, since a discrete system can be viewed as a filter. However, the frequency response provides the accuracy of the discrete system during the steady state; the transient-state accuracy can be analysed by evaluating the pole distortion due to the discretization. This work focuses on the analysis of the steady-state accuracy and the transient-state accuracy of two discrete systems: an RL branch used as a first order system and an RLC branch used as a second order system. For this analysis, two commonly used discretization rules are considered, backward Euler and trapezoidal rules.

Frequency response, Integration rule, time step, backward Euler, Trapezoidal rule

Resumen

La selección de regla y del paso de integración (Δt) es primordial para asegurar resultados precisos en la simulación de una red eléctrica. Por esta razón, este trabajo tiene como objetivos analizar la distorsión que sufren las formas de onda obtenidas debida a la regla y al paso de integración, y proporcionar directrices que ayuden a los usuarios de simuladores de redes eléctricas en la selección adecuada de estos elementos acuerdo a cierta precisión deseada. Al aplicar una regla de integración a un sistema, se puede utilizar su respuesta en frecuencia para evaluar la precisión de dicha regla, ya que un sistema discreto se puede analizar como un filtro. Sin embargo, la respuesta en frecuencia proporciona solamente la precisión de la respuesta de estado estable; la precisión de la respuesta transitoria se puede analizar mediante la evaluación de la distorsión que sufren los polos de los sistemas continuos cuando se convierten a discretos. Este trabajo se centra en los análisis de las precisiones de estado estable y estado transitorio de dos sistemas discretos: una rama RL serie como sistema de primer orden y una rama RLC serie como sistema de segundo orden. Para este análisis se utilizan la regla trapezoidal y Euler hacia atrás, dos de las reglas de integración más utilizadas para la simulación de redes eléctricas.

Respuesta en frecuencia, Regla de integración, Euler hacia atrás, Regla trapezoidal

Citation: GALVÁN-SÁNCHEZ, Verónica Adriana, BAÑUELOS-CABRAL, Eduardo Salvador, GARCÍA-SÁNCHEZ, Jorge Luis and SOTELO-CASTAÑÓN, Julián. Precision analysis of the integration rules used for transient simulation in electric networks. Journal of Technological Operations. 2023. 7-19: 1-11

* Author Correspondence (e-mail: veronica.galvan@academicos.udg.mx)

† Researcher contributing as first author.

Introduction

Transient analysis calculates the response of a circuit as a function of time by numerically integrating the set of differential equations that model the system or by modeling the voltage and current relationships of each element. These relationships are represented by equivalent circuits consisting of combinations of resistors and sources whose values depend on the integration rules used. This is the approach used in electromagnetic transient simulators such as EMTP and SPICE, which are widely used computer programs for the study of transients in power systems [1].

The accuracy of the integration rules used to simulate transients has been studied extensively using the frequency response of an inductor or capacitor in [2]-[3]; however, a power network can be viewed as a combination of multiple first- and second-order branches. This paper focuses on the analysis of the steady-state and transient-state accuracies of two discrete systems: a series RL branch as a first-order system and a series RLC branch as a second-order system. The trapezoidal and backward Euler rules, two of the most widely used integration rules for the simulation of electrical networks, are used for this analysis.

Integration Rules for Electromagnetic Transient Simulation

Two of the most commonly used integration rules in electrical network simulation are backward Euler (BE) and trapezoidal (TRA). These rules are A-stable in that, independent of the accuracy of the solution, they always yield stable results. It is important to note that the accuracy of the response or solution depends on three factors [2]: the inherent properties of the integration rule, the size of the integration step, and the characteristics of the circuit being simulated.

Discretization procedure

The discrete equivalent $H[z]$ of a continuous transfer function $H(s)$ can be obtained by mapping from the s-domain to the z-domain. For the cases of the integration rules used in this paper, the mapping is performed by the following formulas [3]:

$$s_{TRA} = \frac{2}{\Delta t} \frac{z-1}{z+1}, \quad s_{BE} = \frac{1}{\Delta t} \frac{z-1}{z}, \quad (1a), (1b)$$

where Δt is the time increment or integration step.

Accuracy of integration rules

The frequency response of a system provides the steady-state response to sinusoidal inputs over a frequency range. When the system is in steady state, the output differs from the input only in magnitude and phase. For this reason, the accuracy of a discrete system $H[z]$ can be evaluated by comparing its frequency response with the frequency response of the continuous system $H(s)$. To obtain the frequency response of $H(s)$, the complex frequency is sampled as

$$s = j2\pi k \Delta f, \quad k = 0, 1, 2, \dots, N-1 \quad (2)$$

where Δf is the frequency increment and N is the number of samples. Note that $(N-1) \Delta f$ is the maximum frequency or Nyquist frequency f_{Ny} . To obtain the frequency response of $H[z]$, $z = e^{s\Delta t}$ is used, where s is sampled as in (2) and $\Delta t = 1/(2f_{Ny})$. The frequency responses in this article are plotted using a normalized frequency

$$\text{Normalized frequency} = \frac{s}{j2\pi F_s} (\text{pu}), \quad (3)$$

which is defined as the frequency per unit of the sampling frequency $F_s = 2f_{Ny}$. The normalized frequency has a range from 0 to 0.5, where 0.5 is the normalized f_{Ny} .

This paper also analyzes the errors of the natural response of discrete systems. To perform this analysis, the poles and residues of discrete systems are compared with those of continuous systems; the comparison is performed in the continuous plane. For this, the discrete parameter in question is converted to a distorted parameter that exists in the continuous domain; for example, a discrete $p_{discrete}$ pole is converted to a distorted $p_{distorted}$ pole using the formula [4].

$$p_{distorsionado} = \ln(p_{discreto}) / \Delta t \quad (4)$$

First Order System

The first-order system considered in this article is an RL branch. Taking voltage as input and current as output, $H(s)$ is the transfer function of the continuous system, which is

$$H(s) = \frac{1/L}{s + R/L}. \quad (5)$$

Substituting (1) into (5) gives the following discrete transfer functions:

$$H_{TRA}[z] = \frac{\Delta t}{R\Delta t + 2L} \frac{z+1}{z + (R\Delta t - 2L)/(R\Delta t + 2L)}, \quad (6a)$$

$$H_{BE}[z] = \frac{1}{R + L/\Delta t} \frac{z}{z - 1/(R\Delta t/L + 1)} \quad (6b)$$

The impulse response of the first-order system has the form $h(t) = re^{pt}$, where r and p are respectively the residue and pole of (5). From (6) we obtain the impulse responses as in [5], which have the form

$$h[m] = \left\{ (r_{discrete}) (p_{discrete})^{m\Delta t} + k_{discrete} [0] \right\} / \Delta t \quad (7)$$

$$m = 0, 1, 2, \dots, N-1, m$$

where $r_{discrete}$, $p_{discrete}$ and $k_{discrete}$ are respectively the residue, the pole and the constant term of (6); note that the values of these parameters are different for (6a) and for (6b).

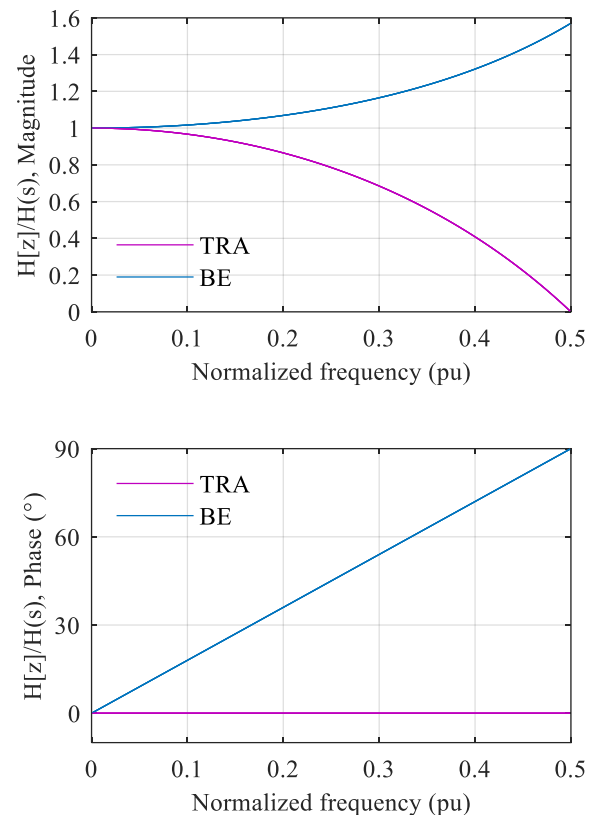
Accuracy of the steady state solution

The accuracy of some integration rules is presented in [1]. In this reference, the frequency response of a pure inductance is considered, which is reproduced in graph 1. The curves in graph 1 depend only on the Δt and the integration rule, which means that they do not depend on the circuit parameters (L in this case). However, this is not the case for circuits that are composed by a variety of elements as shown below. In the case of the RL branch, different plots are obtained for different values of R , L and Δt . To obtain standard shape curves as in graph 1, the Δt is defined in a general way, i.e., for any value of R and L . This time increment can be specified by the bandwidth of the system represented by (5). Although this system is not band-limited, most of the spectrum energy is contained in a band from $f = 0\text{Hz}$ to $f = B\text{Hz}$. For example, the bandwidth B containing 90% of the spectrum energy can be obtained by the energy criterion [6].

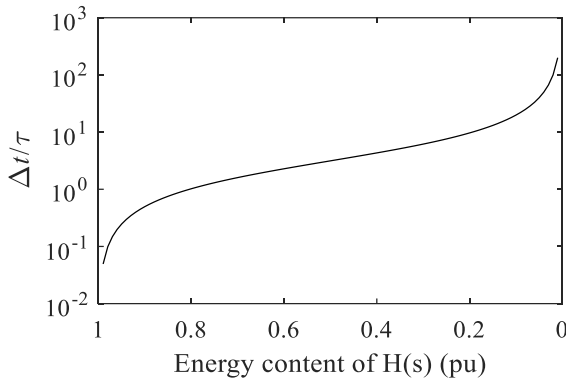
$$B = \frac{|p| \tan(0.90\pi/2)}{2\pi}. \quad (8)$$

The criterion for selecting B depends on the tolerance error of each specific application [6]. It is worth mentioning that to select the Δt according to B , $\Delta t = 1/(2B)$ is used, i.e., $B = f_{Ny}$. Graph 2 shows the effect of energy content on the normalized Δt ; the time constant of the system ($\tau = L/R$) is used as the time base.

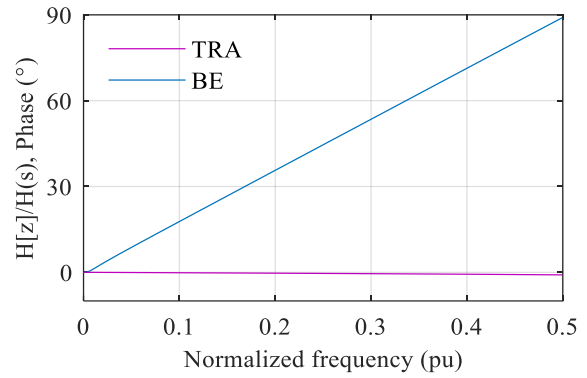
Graph 3a presents the frequency response of the first order discrete system if f_{Ny} (B) is selected to contain 90% of the spectrum energy. Unlike the case of a pure inductance, it can be noticed in this graph that the RL system discretized by TRA presents error in the phase; however, this discrete system has less than 5% error in amplitude and only one degree of error at a frequency equal to one fifth of f_{Ny} , while the errors of the system discretized by BE are considerably larger at that same frequency. If f_{Ny} is selected so that it contains 99% of the energy of the spectrum, the frequency responses are as shown in graph 3b. Similar to the case of pure inductance, the phase error for TRA is negligible over the entire frequency range.



Graph 1 Comparison of the frequency response of the discrete systems versus the continuous system

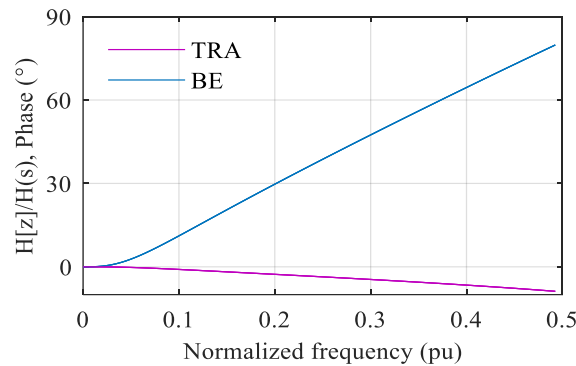
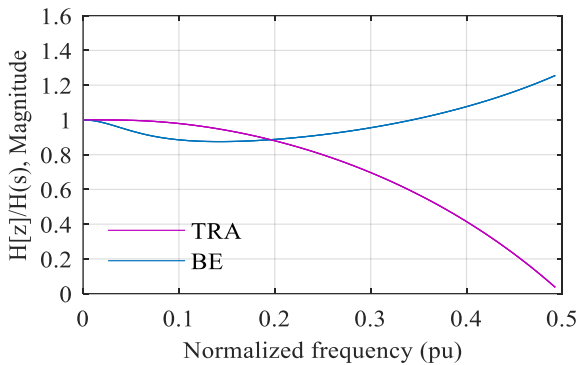


Graph 2 Variation of Δt as a function of the energy content of the first-order system spectrum

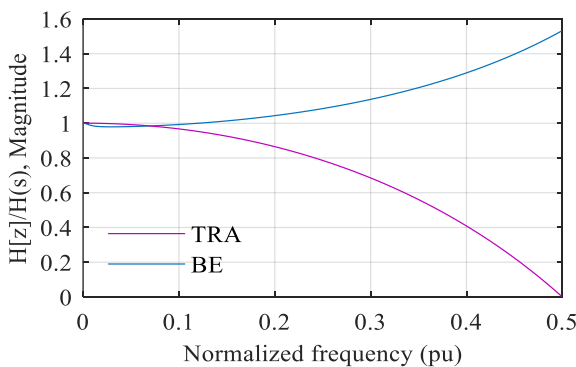


Graph 3 B

Graphic 3 Frequency response of first order systems if the Δt is calculated with the energy criterion; with (a) 90% of the spectrum energy, (b) 99% of the spectrum energy.

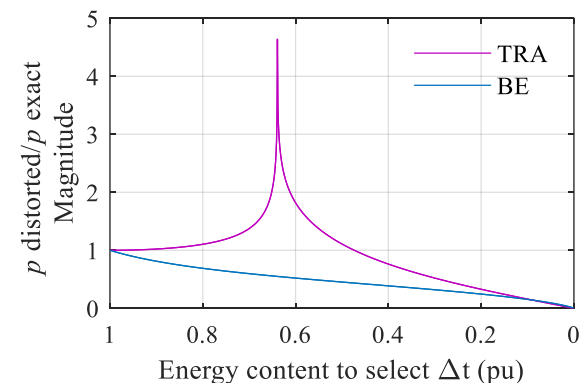


Graph 3 A

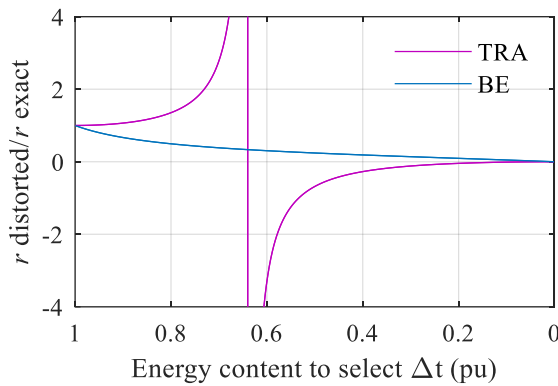


Accuracy of the transient solution

To discretize the continuous system, the Δt is varied according to a variation of the energy content of the spectrum of (5) from 0.1% to 99.9% (0.001pu to 0.999pu). The poles and distorted residuals are compared with the exact values in graph 4. This plot is standard for any first-order system if the Δt is chosen according to the energy criterion. At the Δt corresponding to approximately 64% (0.64 pu) of the energy there is a resonance in the plot. This resonance is due to the fact that from this Δt the pole and the discrete residue become negative; in the continuous plane the distorted magnitudes become complex. Graph 4a shows that with a Δt corresponding to 90% of the energy, the error of the TRA distorted pole is 2.1% while the BE distorted pole is 18.8%. From graph 4b it can be seen that TRA always overestimates the magnitudes of the residues when the distorted pole is real, while BE underestimates them. With a Δt corresponding to 90% of the energy, the error of the residue distorted by TRA is less than 10%, while the error of the one distorted by BE is greater than 30%.



Graph 4 A



Graph 4 B

Graphic 4 Comparison of the distorted poles and residuals of the first order system against the exact values. (a) Comparison of the distorted poles, (b) comparison of the distorted residuals

Second order system

A series RLC circuit is used to evaluate the steady state response and transient response of a second order system. To obtain different damping factors ζ , the resistance R is varied in the following equation:

$$\zeta = \frac{R}{2} \sqrt{\frac{C}{L}}, \quad (9)$$

Since when simulating low ζ transients, the frequency and damping of the natural response strongly depend on the time increment and the integration rule. Transfer function $H(s)$ of the RLC branch is used as a reference to compare the different numerical methods. If the source voltage is taken as input and the voltage on the capacitor as output, the transfer function of the RLC branch is

$$H(s) = \frac{1/(LC)}{s^2 + (R/L)s + 1/(LC)}. \quad (10)$$

Substituting (1) into (10), we obtain the discrete transfer functions

$$H_{TRA}[z] = \frac{1/(LC)}{\left(\frac{2}{\Delta t} \frac{z-1}{z+1}\right)^2 + \frac{R}{L} \left(\frac{2}{\Delta t} \frac{z-1}{z+1}\right) + \frac{1}{LC}} \quad (11a)$$

$$H_{BE}[z] = \frac{1/(LC)}{\left(\frac{1}{\Delta t} \frac{z-1}{z}\right)^2 + \frac{R}{L} \left(\frac{1}{\Delta t} \frac{z-1}{z}\right) + \frac{1}{LC}} \quad (11b)$$

The impulse response $h(t)$ of the second-order system in (10) has the form $h(t) = r_1 e^{p_1 t} + r_2 e^{p_2 t}$, where the variables r and p are respectively the residues and poles of (10). From (11) we obtain the impulse responses of the discrete systems, which have the form

$$h[m] = \left\{ \left(r_{discrete,1} \right) \left(p_{discrete,1} \right)^{m\Delta t} + \left(r_{discrete,2} \right) \left(p_{discrete,2} \right)^{m\Delta t} + k_{discrete} [0] \right\} / \Delta t$$

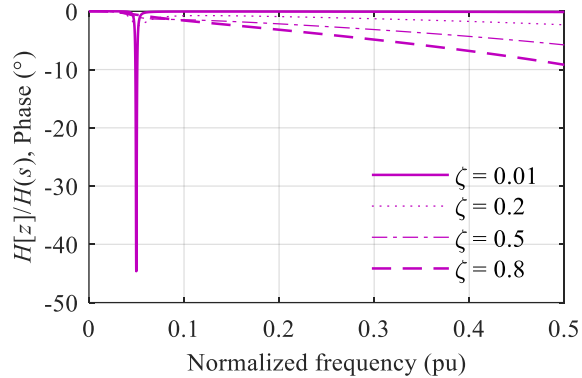
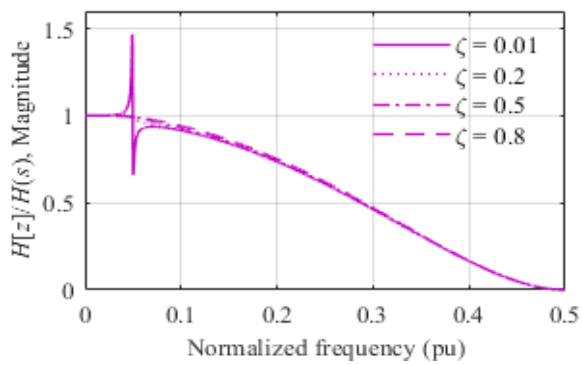
$$m = 0, 1, 2, \dots, N-1 \quad (12)$$

where the variables $r_{discrete}$, $p_{discrete}$ and $k_{discrete}$ are respectively the residues, the poles and the constant term of (11); note that the values of these parameters are different for (11a) and for (11b).

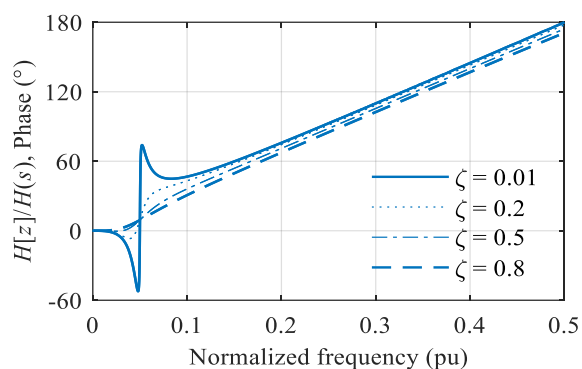
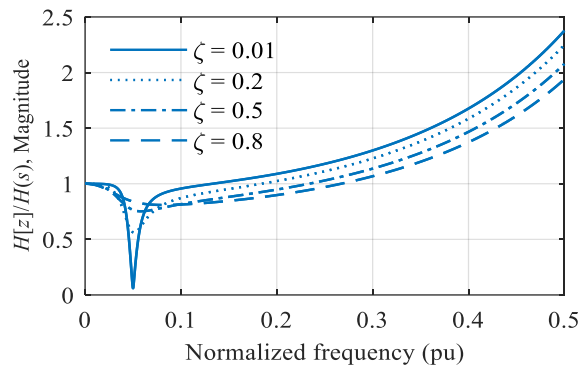
Accuracy of the steady state solution

For the underdamped case, systems with damping factors 0.01, 0.2, 0.5 and 0.8 are analyzed, and for the overdamped case, systems with damping factors 1.1, 5 and 10 are analyzed. The critically damped case, i.e., the system with $\zeta=1$, is also included. *Underdamped system.* If $f_{Ny} = 10f_0$ ($\Delta t = 0.05T_0$), is chosen, the comparisons of the frequency responses are as found in graphs 5a and 5b. It is pertinent to clarify that the error in magnitude of TRA around the resonance frequency ($f_{Ny}/10$) is due to the phase shift of the frequency response [7].

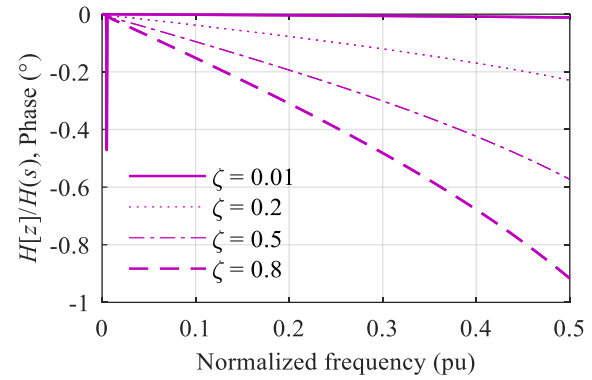
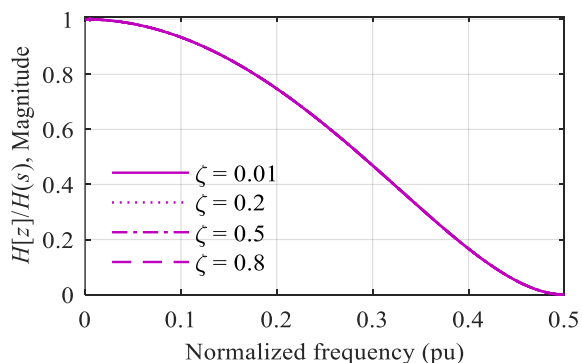
What happens in the case of BE discretizations is different: the magnitude of the frequency response is significantly attenuated around f_0 for all damping factors; the phase of the response is also highly distorted around the resonance frequency. If f_{Ny} is increased so that it is $100f_0$ ($\Delta t = 0.005T_0$), the frequency responses are as in graphs 5c and 5d. In this case, the error in magnitude around the resonant frequency for all considered values of ζ is negligible for TRA, but is considerable for BE when $\zeta = 0.01$. The error in the TRA phase is less than 1° for the whole frequency range, and for BE the error has an almost linear behavior (from 0 to 180°) over the whole frequency range, except around f_0 .



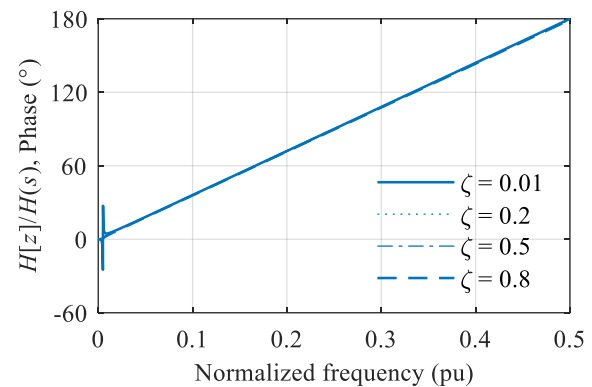
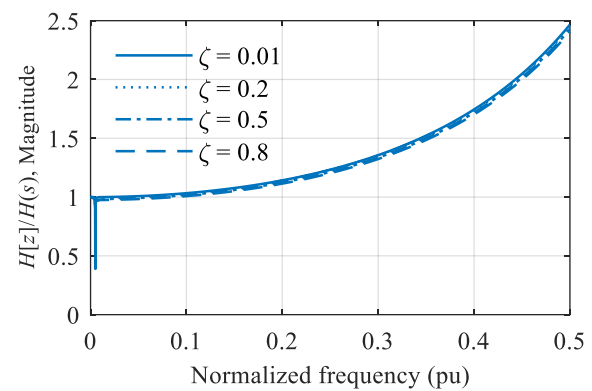
Graph 5 a



Graph 5 b



Graph 5 c



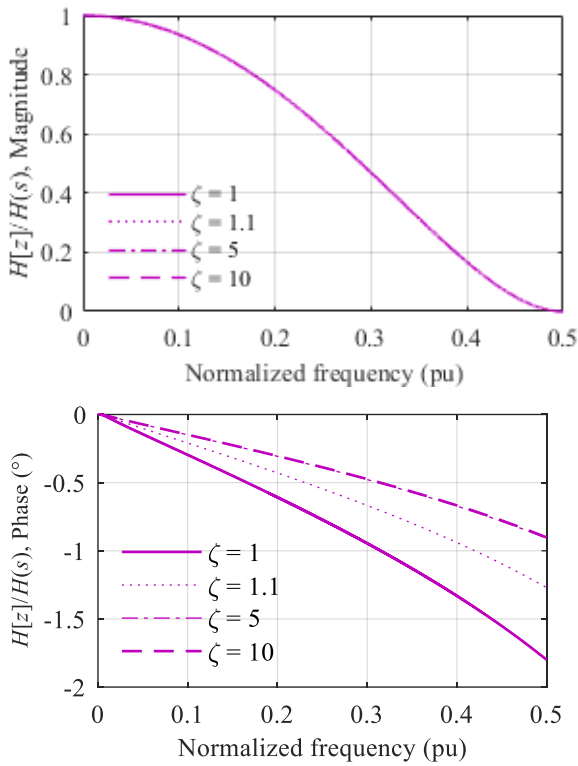
Graph 5 d

Graphic 5 Comparison of frequency response of underdamped second order systems. (a) TRA discretized systems with $f_{Ny} = 10f_0$, (b) BE discretized systems with $f_{Ny} = 10f_0$, (c) TRA discretized systems with $f_{Ny} = 100f_0$, (d) BE discretized systems with $f_{Ny} = 100f_0$.

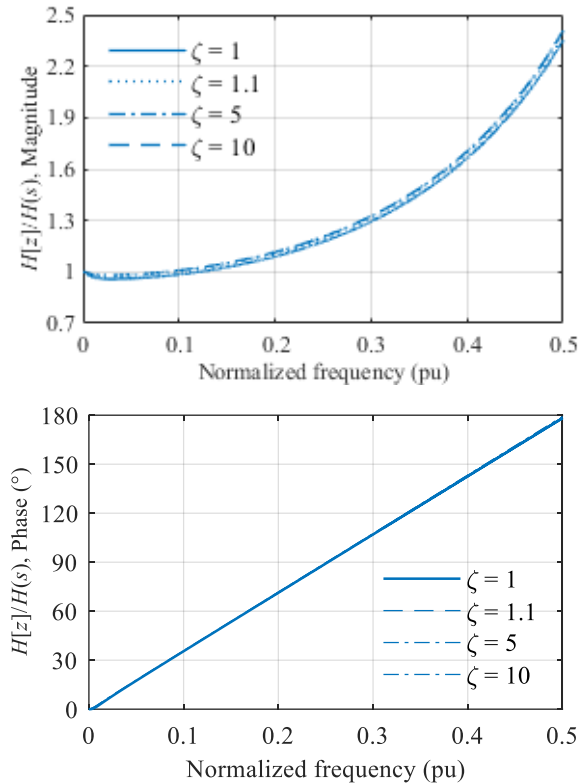
Critically damped and overdamped systems

The comparison of the frequency response of discrete and analytical systems is shown in graph 6. f_{Ny} used for the analysis corresponds to 99% of the energy. For all the systems discretized by TRA, the error in the magnitude of the response is less than 2% for sources whose frequency is up to one tenth of f_{Ny} ; in the same frequency range, the error of the steady state response in the phase is less than half a degree. It can be seen that with BE the error in the response amplitude is smaller than with TRA, however, the error in the phase of BE is very large; for example, for a source frequency of one-fifth of f_{Ny} , the error is greater than 30° .

GALVÁN-SÁNCHEZ, Verónica Adriana, BAÑUELOS-CABRAL, Eduardo Salvador, GARCÍA-SÁNCHEZ, Jorge Luis and SOTELO-CASTAÑÓN, Julián. Precision analysis of the integration rules used for transient simulation in electric networks. Journal of Technological Operations. 2023



Graph 6 a



Graph 6 b

Graphic 6 Comparison of the frequency response of critically damped and overdamped second order systems for a Δt corresponding to 99% of the energy. (a) Discrete system using TRA, (b) Discrete system using BE.

Accuracy of the transient state solution

To make comparisons of the discrete system parameters with the analytical system parameters, the damping factor is varied from 0.01 to 0.99 and the Δt to discretize the continuous systems is varied from 0.1 to 0.0017 times the period of the resonance frequency T_0 ; in other words, the T_0 is varied from 5 to 300 times the resonance frequency f_0 .

Underdamped system

The impulse response $h(t)$, with $p_1, p_2 = \sigma \pm j\omega_n$ and $r_1, r_2 = A/2 e^{\pm j\theta}$ has the form of a damped cosine and can be expressed in the following ways.

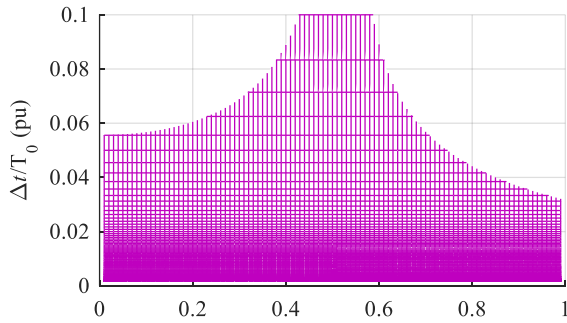
$$\begin{aligned} h(t) &= r_1 e^{p_1 t} + r_2 e^{p_2 t} = A e^{\sigma t} \cos(\omega_n t + \theta) \\ &= 2|r_1| e^{\Re\{p_1\}t} \cos(\Im\{p_1\}t + \angle r_1) \end{aligned} \quad (13)$$

In the underdamped case, r_1 and r_2 as well as p_1 and p_2 are complex conjugates respectively. The imaginary part of p_1 is considered to be positive and therefore r_1 contains θ , the cosine phase. The mapping of s to the z -plane distorts the real part and the imaginary part of a complex number differently [4]. For this reason, the accuracy analysis is performed on the following parameters of the impulse response: $\omega_n = \Im\{p_1\}$, $\sigma = \Re\{p_1\}$, $A = 2|r_1|$, $\theta = \angle r_1$. The graphs are left as a sheet and a cut is made to show minimum precisions.

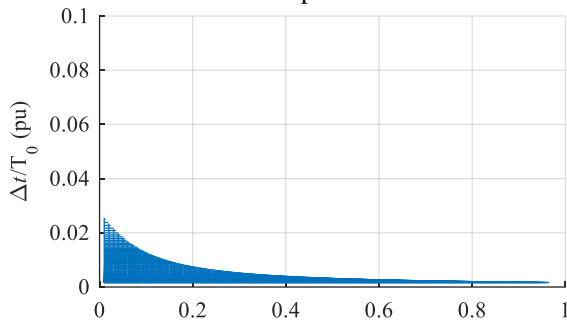
Graph 7 shows comparisons of the natural frequency ω_n and damping σ with their exact equivalents at 99% minimum accuracy. Graphs 7a and 7c illustrate that when discretizing by TRA and using a $\Delta t = 0.03T_0$, the accuracy of both ω_n and σ is at least 99% for all damping factors; in contrast, Graphs 7b shows that when discretizing by BE and using a $\Delta t = 0.01T_0$, only damping factors smaller than 0.1 can be represented with 99% minimum accuracy. Using BE, Graph 7c shows that the smallest damping factor that can be used such that the 99% minimum accuracy of σ is obtained is $\zeta = 0.37$; to achieve this accuracy the smallest Δt considered in this work, 0.0017 s, must be used.

Graph 8 shows the comparisons for the amplitude of the response A and the phase of the discrete systems θ . The sheets present a cutoff so that a minimum accuracy of 99% is shown.

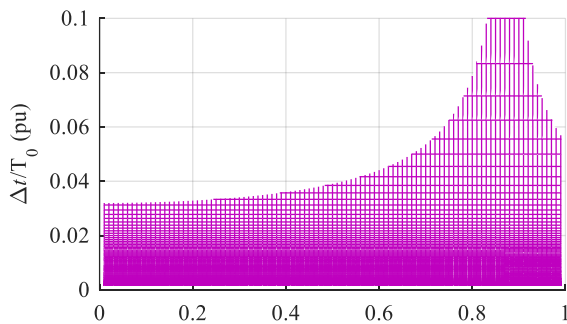
With TRA, similar to the behavior of ω_n and σ , when using a maximum time increment $\Delta t = 0.03T_0$, the accuracy in A is at least 99% for all damping factors. With BE the time increments must be much smaller to reach 99% accuracy for all damping factors.



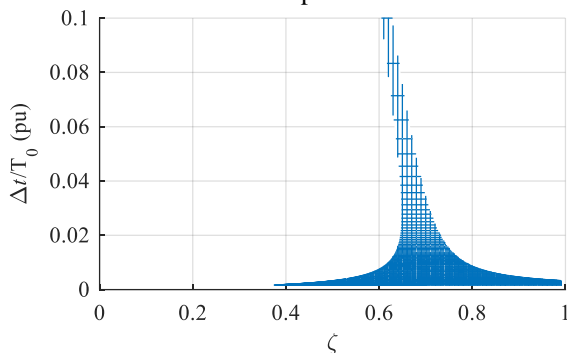
Graph 7 a



Graph 7 b



Graph 7 c

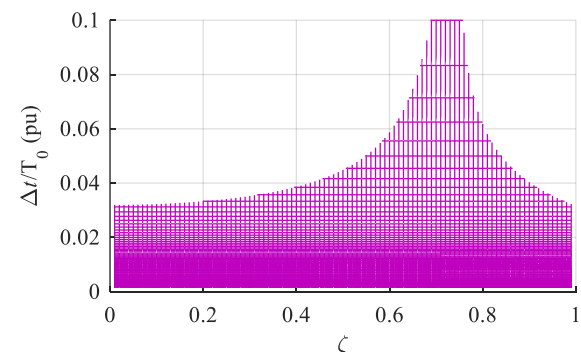


Graph 7 d

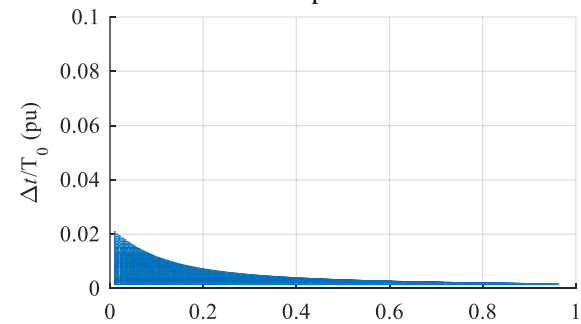
Graph 7 (a) $\omega_n, \text{distorted}/\omega_n, \text{exact}$, TRA; (b) $\omega_n, \text{distorted}/\omega_n, \text{exact}$, BE; (c) $\sigma_{\text{distorted}}/\sigma_{\text{exact}}$, TRA; (d) $\sigma_{\text{distorted}}/\sigma_{\text{exact}}$, BE.

For TRA, with an approximate maximum time increment $\Delta t = 0.04T_0$, the accuracy θ is within the mentioned accuracy range for all damping factors considered. It is very interesting to note that for BE the error with all time increments for all damping factors considered is zero, i.e., from this it can be concluded that the phase of the natural response is not affected by the application of BE.

Overdamped system. The two real poles of the second order system have different time constants. To choose the appropriate time step using the energy criterion, the appropriate bandwidth B is selected according to the faster pole (the one with the larger absolute value). The behavior of the faster pole is seen as in the Graph of the first-order system in Graph 5. The other pole, whose bandwidth is smaller, possesses higher accuracy for the specified Δt .

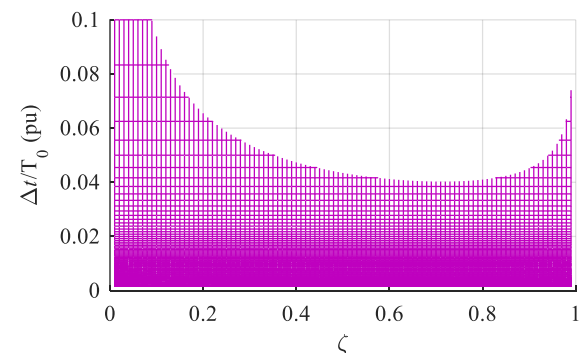


Graph 8 a

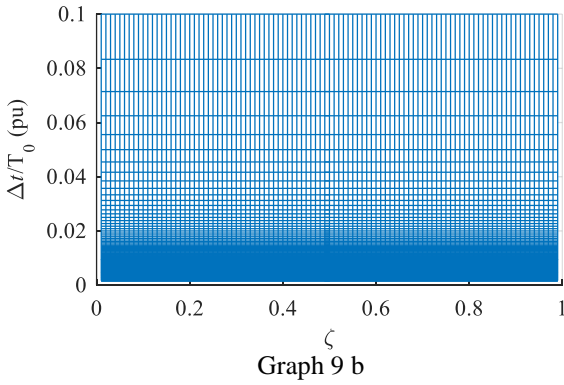


Graph 8 b

Graph 8 (a) $A_{\text{distorted}}/A_{\text{exact}}$, TRA; (b) $A_{\text{distorted}}/A_{\text{exact}}$, BE; (c) $\theta_{\text{distorted}}/\theta_{\text{exact}}$, TRA; (d) $\theta_{\text{distorted}}/\theta_{\text{exact}}$, BE



Graph 9 a



Graph 9 $\theta_{\text{distorted}}/\theta_{\text{exact}}$, (a) TRA, (b) BE. Comparisons show 0.1° maximum error

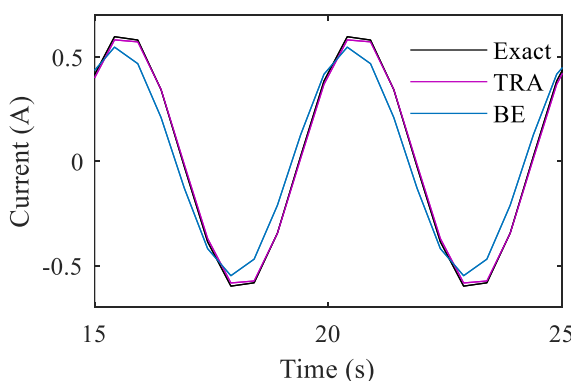
Results and discussions

In order to verify the accuracy analysis presented in the previous section, time domain simulations of the first and second order systems are performed.

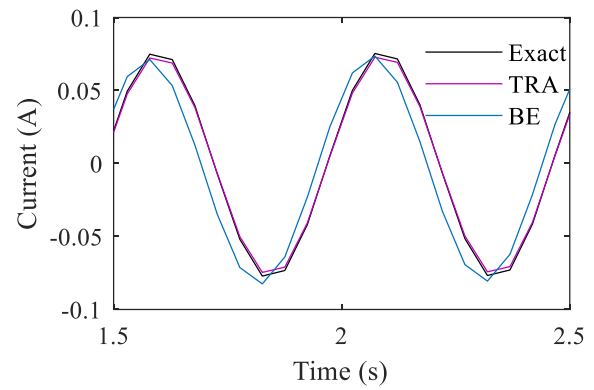
Series RL circuit

The impulse response and the response to a sinusoidal input of a series RL circuit are analyzed. $R = 1\Omega$ and $L = 1H$ are used in this case, so that the time constant of the system is $\tau = L/R = 1$ s.

To evaluate the accuracy during steady state for a sinusoidal input, a voltage source with frequency equal to one fifth of the f_{Ny} and amplitude of 1 V is used. The f_{Ny} , and hence the Δt , is calculated with two different bandwidths, corresponding to 90% and 99% of the energy of the system transfer function. When using the f_{Ny} corresponding to 90% of the energy, it can be seen in Graph 10a that the accuracy of BE is very poor, as predicted in Graph 3a, which presents the frequency response; in the case of Graph 10b, the accuracy in the magnitude of BE is higher than TRA, as shown in 3b, however, the response is leading by more than 15° .



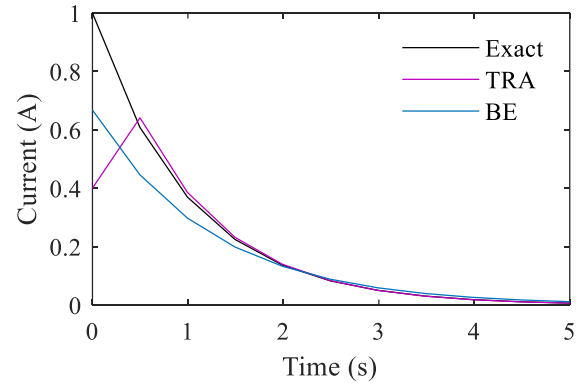
Graph 10 a



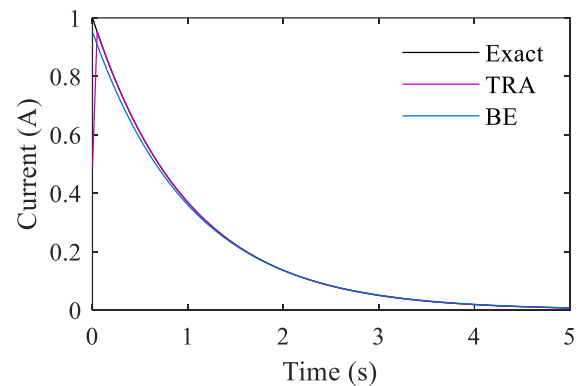
Graph 10 b

Graph 10 Comparison of the steady-state response of the first-order system for a source with frequency $f = f_{Ny}/5$; $f = f_{Ny}/5$ is calculated with (a) 90% of the signal energy, (b) 99% of the signal energy

The accuracy of the transient response of discrete systems is evaluated by their impulse response. The time increments used to apply the integration rules are obtained with 90% and 99% of the signal energy. In order to evaluate the behavior up to the steady state, the responses are plotted with a duration of 5τ , i.e. 5s. Graph 11 shows the solution of the system with the two integration rules.



Graph 11 a



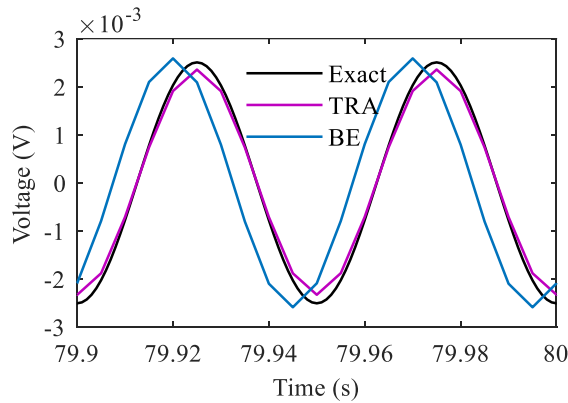
Graph 11 b

Graph 11 Comparison of impulse response of discrete systems with analytical. (a) Impulse responses with Δt corresponding to 90% of the signal energy, (b) Impulse responses with Δt corresponding to 99% of the signal energy

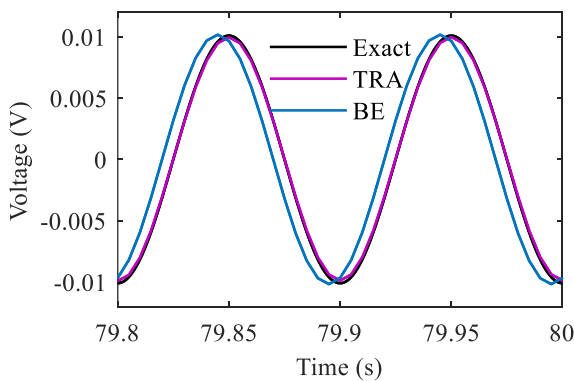
Series RLC circuit

The values of inductance L and capacitance C are taken as $0.5/\pi$ so that the circuit has a resonant frequency $f_0 = 1$ Hz or $\omega_0 = 2\pi$ rad/s. The period of the resonant frequency is $T_0 = 1/f_0 = 1$ s. *Underdamped case:* the most critical case considered in this work is used, which is the system with $\zeta = 0.01$. Graph 12 shows the steady state solution of the second order system if a time increment $\Delta t = T_0/200 = 0.005T_0 = 0.005$ s is used or, in other words, if $f_{Ny} = 100f_0 = 100$ Hz. Two solutions are presented corresponding to the use of two sources with frequencies of $f_{Ny} = 100f_0 = 100$ Hz and $f_{Ny}/10$ (10 Hz). The Graph s show the solution at times close to the 5 time constants.

Graph 12a shows that the BE accuracy is very poor in both magnitude and phase; the solution with TRA is in phase and only slightly attenuated. In Graph 12b it can be seen that the magnitude of the solution with BE is slightly closer to accurate than with TRA (as predicted in Graph 5b), however, the phase is leading.



Graph 12 a



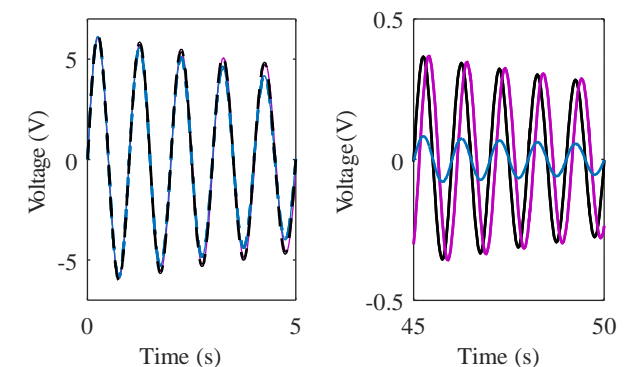
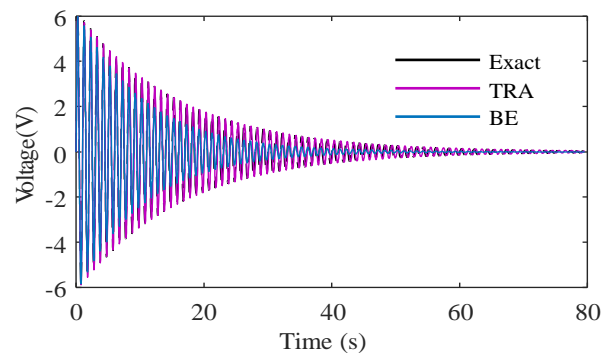
Graph 12 b

Graph 12 Steady state solution of a second order system with $\zeta = 0.01$, (a) $f_{Ny}/5$, (b) $f_{Ny}/10 = 100f_0$ and with the source at the following frequencies (a) $f_{Ny}/5$, (b) $f_{Ny}/10$.

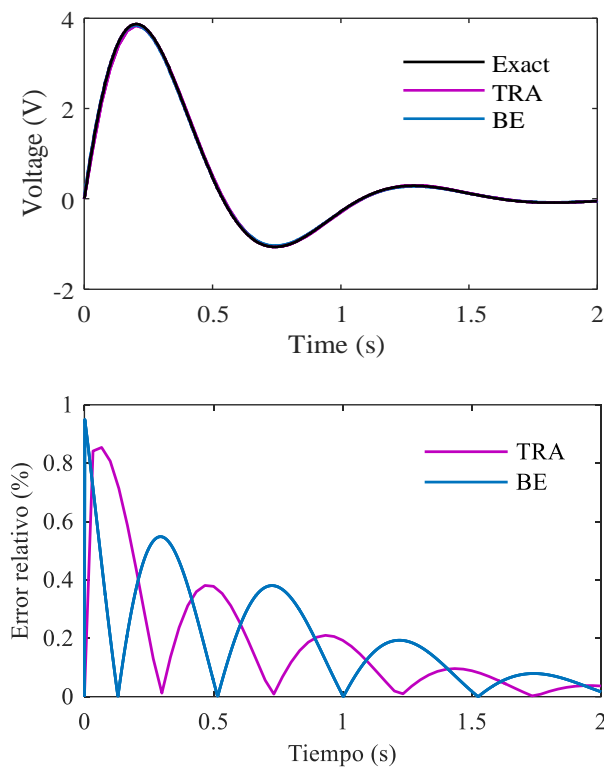
To solve for the transient state of the system, the maximum Δt is chosen from Graphs 7-9 so that the natural response parameters are at least 99% accurate. For TRA, the value is $\Delta t \approx T_0/32 \approx 0.0313T_0 \approx 0.03125$ s; for BE the minimum Δt considered, $\Delta t = T_0/600 \approx 0.00167$ s is used; this Δt does not guarantee 99% accuracy in the σ parameter.

The exact and numerical impulse responses are presented in Graph 13. Regarding the solution with TRA, one can observe a shift of the solution with respect to the analytical one that looks like a phase shift; however, this error is due to the error in the natural frequency ω_n and is not an error in the phase. It can be seen in Graph 9a that for the ζ and Δt used, the error in phase is less than 0.1° . What occurs in the BE solution is excessive attenuation; the oscillations remain in phase with the analytical solution.

This error is due to the fact that BE underestimates the value of σ (overestimates the absolute value), which causes the natural response to decay more rapidly.



Graph 13 Impulse response of the second-order system with $\zeta = 0.01$. For TRA a $\Delta t \approx 0.03125$ s is used and for BE a $\Delta t \approx 0.00167$ s is used



Graph 14 Impulse response and relative error of the second-order system with $\zeta = 0.01$. For TRA $\Delta t \approx 0.03333$ ($f_{Ny} = 15f_0$) and for BE a $\Delta t \approx 0.00167$ s ($f_{Ny} = 300f_0$) is used

If BE is used and a Δt considered in this work ($\Delta t \approx 0.00167$ s), the system with $\zeta = 0.38$ is the case with the smallest ζ that meets the 99% accuracy in all its parameters (see Graphs 7-9). To obtain similar accuracy with TRA, the chosen time increment is $\Delta t \approx 0.0333$ s. The impulse responses and relative error are presented in Graph 14 for both BE and TRA. The relative error is defined, with the magnitude of the analytical damped cosine (A_{exact}) instead of the maximum value of $h(t)$.

Conclusions

This paper presents an analysis of the accuracy of a first order and a second order system when they are discretized by backward Euler and trapezoidal rule. This analysis is intended to guide new users of electromagnetic transient simulators in the proper choice of the integration step, since the size of the integration step affects the accuracy of the simulation. It was observed in this work that the appropriate time step size depends not only on the maximum frequency of the phenomenon to be observed as mentioned in [3], [8], but also on the damping factor of the systems.

As future work, based on this work it is proposed to automatically choose a suitable time increment according to the accuracy set by the user. This would be possible if the eigenvalues of the system to be simulated are known in advance; programs such as Simulink [9] can provide such eigenvalues.

References

- [1] J. A. Hollman, "Real time distributed network simulation with pc clusters. Ph.D. dissertation," Dept. Elect. Comput. Eng., Univ. British Columbia, Vancouver, BC, Canada, 1999. NODA, Taku; TAKENAKA, Kiyoshi; INOUE, Toshio. "Numerical integration by the 2-stage diagonally implicit Runge-Kutta method for electromagnetic transient simulations." IEEE Transactions on Power Delivery, 2009, Vol. 24, No. 1, pp. 390-399.
- [2] Ken Kundert, The Designer's Guide to Spice and Spectre®, Springer Science & Business Media, 2006.
- [3] J. R. Martí and J. Lin, "Suppression of numerical oscillations in the EMTP," IEEE Trans. Power Systems, vol. 4, pp. 739-747, May 1989.
- [4] Rahkonen, Timo, and Pietro Andreani. "Numerical effects in time-domain simulations of electronic circuits-a reminder." NORCHIP Conference, 2005. 23rd. IEEE, 2005.
- [5] J. G. Proakis and D. G. Manolakis, Digital Signal Processing, 4th ed., Prentice Hall, 2006, pp. 195-196.
- [6] B. P. Lathi, Linear Systems and Signals, Oxford University Press, 2009.
- [7] Galván, V. A.; Martí, J. R.; Dommel, H. W.; Gutiérrez-Robles, J. A.; Naredo, J. L. "MATE multirate modelling of power electronic converters with mixed integration rules". Power Systems Computation Conference (PSCC), 2016.
- [8] De Siqueira, J. C.; Bonatto, B. D.; Martí, J. R.; Hollman, J. A.; Dommel, H. W. "A discussion about optimum time step size and maximum simulation time in EMTP-based programs". International Journal of Electrical Power & Energy Systems, 2015, 72, pp. 24-32.
- [9] Matlab 2015b, The MathWorks, Inc., Natick, Massachusetts, United States.

Maintenance management of pneumatic equipment and facilities at a plant in the Industrial corridor in the South area of the state of Tamaulipas

Administración del mantenimiento a equipos neumáticos e instalaciones en una planta del corredor Industrial de la zona Sur del estado de Tamaulipas

CRUZ-SUSTAITA, Vianey†*, LERMA-LEDEZMA, David and ESPINOSA-SOSA, Enrique Esteban

Universidad Politécnica de Altamira

ID 1st Author: *Vianey, Cruz-Sustaita* / ORC ID: 0000-0001-6753-7441

ID 1st Co-author: *David, Lerma-Ledezma* / ORC ID: 0000-0001-8137-3308, CVU CONAHCYT ID: 899202

ID 2nd Co-author: *Enrique Esteban, Espinosa-Sosa* / ORC ID: 0009-0002-3100-4226

DOI: 10.35429/JTO.2023.19.7.12.15

Received March 10, 2023, Accepted, June 30, 2023

Abstract

Maintenance planning is focused on production, the work is to limit, avoid and correct failures. The planning is focused on the processes, all maintenance must follow a pre-established and planned process according to the company's maintenance manual. Continuous improvement and planning help to evaluate and improve the execution of maintenance and production in the company. Planning and scheduling are a fundamental part of the proper functioning of maintenance. The development of a company is an organized system that, thanks to the effort and proper functioning of the teams, such as the personnel that work in it; This entire system has an end and is to provide a high-quality service that is competitive at the national level. Each company has a different methodology to manage the maintenance of their equipment and as technology advances, they are renewed for optimum performance. In Altamira, the growth of the companies has been exponential due to a correct administration in their production line, avoiding long delays or inconveniences that affect the company in a monetary way.

Processes, Administration, Production

Resumen

La planeación del mantenimiento está centrada en la producción, el trabajo es para limitar, evitar y corregir fallas. La planeación está centrada en los procesos, todo mantenimiento debe seguir un proceso preestablecido y planificado según el manual de mantenimiento de la empresa. El mejoramiento continuo y la planificación ayuda a evaluar y mejorar la ejecución del mantenimiento y la producción en la empresa. La planeación y la programación forman parte fundamental para el buen funcionamiento del mantenimiento. El desarrollo de una empresa es un sistema organizado que, gracias al esfuerzo y buen funcionamiento de los equipos, como el personal que labora en ella; todo este sistema tiene un fin y es proporcionar un servicio de alta calidad y que a su vez sea competitivo a nivel nacional. Cada empresa cuenta con una metodología diferente para administrar el mantenimiento de sus equipos y conforme va avanzando la tecnología se van renovando para un óptimo desempeño. En Altamira, el crecimiento de las empresas ha sido exponencial debido a una correcta administración en su línea de producción, evitando grandes retrasos o inconvenientes que afecten a la empresa de manera monetaria.

Procesos, Administración, Producción

Citation: CRUZ-SUSTAITA, Vianey, LERMA-LEDEZMA, David and ESPINOSA-SOSA, Enrique Esteban. Maintenance management of pneumatic equipment and facilities at a plant in the Industrial corridor in the South area of the state of Tamaulipas. *Journal of Technological Operations*. 2023. 7-19: 12-15

* Author Correspondence (e-mail: vianey.cruz@upalt.edu.mx)

† Researcher contributing as first author.

Introduction

The industries are an important system within the supply chain since it allows a product of basic necessity to enter the homes of thousands of families that inhabit Mexico.

For this, there is a trained staff that manages to create strategies that make it possible for each product in the basic basket to reach the hands of consumers, calling this a plan.

In the opinion of (Pérez Porto, J., Merino, M, 2009) this plan allows the creation of steps and strategies from the extraction of the raw material to the end of the process, which in this case are the customers who purchase said product.

1. Procedure and Production

Mentioning from (Pérez Porto, J., Gardey, 2008) that procedure is a term that refers to the action that consists of proceeding, which means acting in a certain way.

The concept, on the other hand, is linked to a method or a way of executing something.

A procedure, in this sense, consists of following certain predefined steps to carry out a task efficiently. Its objective should be unique and easy to identify, although it is possible that there are several procedures that pursue the same goal, each with different structures and stages, and that offer more or less efficiency.

From the perspective that is seen in this methodology, the focus of this research is directed to the production area, so it is essential to know about this area.

In the opinion of (Ortega, O, 2019), "The production area plays a very important role in the competitiveness of a company, it is a department that has had to learn to evolve to meet the needs of customers.

It covers all activities that transform raw materials and components into products that will be sold to customers.

The production area describes the entire process by which the company produces a good or service capable of satisfying a demand using factors of production acquired in the market.

2. Production Systems

In the context of a company, the production system, in addition to its primary purpose, which is to produce an economic good, seeks to satisfy other objectives. The production area must allow the company to satisfy the demand that is imposed on it, which means that the company adapts its production capacity to the volume of sales. The economic goods produced must be of good quality, that is, they must satisfy the needs of customers. The production system adopted by the company must offer the lowest possible production costs to guarantee the competitiveness of the company. The system must produce in a reasonable time, that is, according to the level of demand of the company.

There are too many questions about the manufacturing area, however, something important within it is the production system; and depending on the company, the environment changes completely, adapting to the needs that the industry requires to carry out its production correctly, all this because of the type of product that is being made.

This is why it is considered relevant to assimilate about the concept of the production system and everything behind it to make it happen.

"Production systems encompass all the elements that allow raw material to become finished products. Among these factors is, mainly, the administration or management style, the procedures, the machines, the materials, the technologies and, of course, the people or workers." (Munoz, V, 2019)

As can be observed, it is a concept that has a role in all industries, thus allowing the availability of quality articles and goods for the human being.

3. Maintenance

In factories that practice this system, operators and other workers tend to dedicate their efforts to tasks more related to planning, supervision, and maintenance.

Of course, it takes much more than economic resources to make these processes profitable. It is also important that the demand for the manufactured product is high enough, since otherwise it can lead to large losses.

As previously mentioned, it is very important that there is a "planning, supervision and maintenance", which is why, within a company, one of the most important relationships must be the staff and their work area, since day by day there are a series of actions that must be carried out by the personnel within their area, these activities are intended to ensure that the equipment, machines, components and facilities involved in an industrial process are in the required operating conditions for what was designed, built, installed and put into operation.

This series of activities includes a whole combination of knowledge, experience, skill and teamwork, we call this as plan / maintenance.

Taking into account the background of the aforementioned concept, the history of maintenance should be taken as a preamble, which has been and will be very extensive, since over the years and the innovation of technology, new methods have been created., steps or processes that have helped to improve the way in which a piece of equipment receives its respective maintenance. As mentioned, (Olarde C., William; Botero A., Marcela; Cañon A., Benhur, 2010) "The first companies that existed were made up of groups of people who had to work in each of the steps of the production process and in turn repair the tools and machines when they had a breakdown.

Because the workers developed multiple trades, producing a finished product to offer it to the market implied a high cost in time and money. With the objective of earning more, investing less, the companies were forced to distribute their workers to dedicate themselves to specific tasks, these tasks were of two types: Machine operation tasks and repair tasks. In 1930, the automotive businessman Henry Ford, implemented a new organization system within his company which he called "Chain Production". This new system was established through the assignment of organized responsibilities.

With the new Ford model, the concept of maintenance arose, which depended on the operation department, which was the one that determined when the repair work should be carried out. With World War II, companies had to increase their production to meet market demand; For this, it was necessary to increase their working hours. This hasty way of producing in large quantities and for long periods of time caused the machines to wear out due to excessive use and therefore to fail in their operation.

The repair of the machines implied the stoppage of the production process which generated great losses. In order to avoid these stops, employers gave greater importance to maintenance by restructuring their organizational models. Starting in 1966, with the strengthening of national maintenance associations, he began to develop criteria for failure prediction, thus visualizing the optimization of the performance of maintenance execution teams. In order to carry out a correct procedure, it is necessary to know the equipment in the work area, in this case the investigation is aimed at the pneumatic equipment and facilities, since if it is not known about the history of the machines, there would not be enough information. information, such as failure history, whether maintenance has been performed, economic factors, safety factors; each of these points are valuable when creating the plan.

5. Methodology to develop

For the present research work, tools such as Excel were identified where the maintenance required for the different equipment used could be identified, as well as its brand, model and series with respect to its annual activity.

Breakdowns are expensive because they produce:

- Repair costs that include expenses for materials, personnel expenses, expenses for subcontracted services.
- Damage to machines or facilities, which in some cases means shortening their useful life.

- Production losses, since, on the one hand, the amount of product that has been obtained is lost as a consequence of a malfunction, and on the other, the planning disorder due to late deliveries. But most importantly, bad service if the situation affects customers.
- Risks for people. On some occasions, there are breakdowns that can cause very serious accidents.

Giving with this a follow-up to each of them, as to what maintenance corresponded to them and on what exact date.

The maintenance plan took the following steps: establish objectives, define key performance indicators, take inventory, establish a budget, analyze the available technology, foster a culture and review and optimize.

Results

Maintenance management consisted of maintaining the company's resources so that the operations are carried out effectively and according to the standards and resources, time are not wasted in the work processes when proceeding to carry out some type of maintenance on. With the help of the standards created and the established maintenance calendar that allows to keep track of the tasks that are carried out within the plant. These objectives are to control costs, schedule work adequately and efficiently, and ensure that the company complies with all regulations.



Figure 1 Maintenance
Own Source

Gratitude

We appreciate both the facilities and the information provided by the company located in the industrial area of the port of Altamira.

To the Polytechnic University of Altamira and the Academic Body in Consolidation UPALT-CA-6 "Quality and Productivity".

Conclusions

Throughout this document, the application of a maintenance management procedure is exposed, which is part of the maintenance improvement within the Maintenance Planning and Control department, such a procedure demonstrates the continuous improvement within the plant, not only It should be used if you want to achieve more agile processes by reducing time, but also if you need to reduce any other resource used, obtaining improvements in the productivity of the different tasks to be elaborated.

The results of the implementation allow the plant a comprehensive improvement in quality, reducing costs, optimizing productivity and increasing profitability in the company's operations.

References

- Summer, Donna S.C (2006). Administración de la Calidad.
- Dounce (2009). Villanueva La productividad en el Mantenimiento Industrial.
- Santiago García Garrido (2003). Organización Gestión Integral de Mantenimiento.
- Fred R., David, Conceptos de Administración Estratégicas. 5a Edición, 1997, Pearson Educación, México.

Simulation of the behavior of the flow of electrons between the electrodes of a thermionic converter

Simulación del comportamiento del flujo de electrones entre los electrodos de un convertidor termoiónico

CALVARIO-GONZÁLEZ, Abdías†, BARBOSA-SANTILLÁN, Luis Francisco and JUÁREZ-VARELA, Mirna Patricia

Universidad Tecnológica de Puebla Antiguo Camino A la Resurrección N° 1002 – A Colonia Zona Industrial Oriente Puebla Pue. C.P. 72300

ID 1st Author: Abdías, Calvario-González / ORC ID: 0000-0003-1260-2298, CVU CONAHCYT ID: 68234

ID 1st Co-author: Luis Francisco, Barbosa-Santillán / ORC ID: 0000-0001-6550-0901, CVU CONAHCYT ID: 49306

ID 2nd Co-author: Mirna Patricia, Juárez-Varela / ORC ID: 0009-0001-4175-3231, CVU CONAHCYT ID: 219147

DOI: 10.35429/JTO.2023.19.7.16.30

Received March 10, 2023, Accepted, June 30, 2023

Abstract

Thermionic converters have been shown to be an alternative to generate electrical power from thermal energy, however, efficiency is reduced by its internal impedance. This impedance has not been possible to suppress because thermionic converters require an ionized cesium atmosphere to transport the electrons. Different authors, have proposed alternatives to reduce this impedance, however, this continues being the main limitation to improve the efficiency of thermionic converters. Recently Fitzpatrick et. al have been working with cesium diodes of near spacing which have shown the possibility of decreasing this impedance when working with thermionic converters in Knudsen mode. In this paper, a theoretical analysis of high vacuum thermionic converters based on the fundamental laws of electronic emission is presented. The most important result was the explanation of the curve I vs V of a thermionic diode from its birth to its saturation. And the development of the algorithms that allow the use of the equations that predominantly explain the emission of electrons.

Resumen

Los convertidores termoiónicos han mostrado ser una alternativa para generar potencia eléctrica a partir de la energía térmica, sin embargo, la eficiencia se ve reducida por su impedancia interna. Esta impedancia no ha sido posible suprimirla debido a que los convertidores termoiónicos requieren de una atmósfera de cesio ionizado para transportar los electrones. Diferentes autores, han propuesto alternativas para reducir esta impedancia, sin embargo, continúa siendo ésta la principal limitante para mejorar la eficiencia de los convertidores termoiónicos. Recientemente Fitzpatrick et. al han estado trabajando con diodos de cesio de espaciamiento cercano los cuales han mostrado la posibilidad de disminuir esta impedancia cuando se trabaja con convertidores termoiónicos en el modo Knudsen. En este trabajo se presenta un análisis teórico sobre los convertidores termoiónicos de alto vacío a partir de las leyes fundamentales de emisión electrónica. Se obtuvo como resultado más importante la explicación de la curva I vs V de un diodo termoiónico desde su nacimiento hasta su saturación. Y el desarrollo de los algoritmos que permiten el empleo de las ecuaciones que de manera predominante explican la emisión de electrones.

Simulation, Thermionic, Convert

Simulación, Termoiónico, Convertidor

Citation: CALVARIO-GONZÁLEZ, Abdías, BARBOSA-SANTILLÁN, Luis Francisco and JUÁREZ-VARELA, Mirna Patricia. Simulation of the behavior of the flow of electrons between the electrodes of a thermionic converter. Journal of Technological Operations. 2023. 7-19: 16-30

† Researcher contributing as first author.

Introduction

More than two hundred years ago Du Fay observed that the space surrounding an incandescent body is a conductor of electricity. In 1853 Edmon Becquerel devoted an article to this topic. One of the observations he published was that a potential of a few volts was sufficient to make current flow into a galvanometer that closed the circuit with the hot air between the red-heated platinum electrodes.

Between the years 1882 to 1889 Elster and Geitel worked on a sealed device containing two electrodes, one that could be heated and one that could be cooled; they noted by means of an electrometer connected to the cold electrode that charge flowed from the hot electrode to the cold electrode; they also found that at relatively low temperatures the current passed more easily if the hot filament was positively charged. At moderately high temperature; they noted that; charge could be transferred just as easily from the hot filament to the cold filament as from the cold filament to the hot filament. At higher temperature they noted that the negatively charged filament predominated.

In 1883 in a patent application, Thomas Alva Edison stated that he observed the thermionic effect in a vacuum. Seven years later, Preece and Fleming demonstrated that the thermionic effect was due to electric flux leaving the main filament, passing through the vacuum, and collecting at the relatively positive electrode.

The nature of the negative charge carriers was determined until 1899 by J.J. Thomson, who found that the ratio of charge to mass agreed with the value he found for the electron.

Basically the thermionic effect consists of the emission of electrons that are generated in a hot electrode with respect to a cold electrode that collects it. The former is called emitter and the latter collector. According to reports, this phenomenon occurs in materials at temperatures above 1000 K.

To explain this phenomenon, it is necessary to be clear about the concepts of Fermi level and work function.

The Fermi level of a material is defined as the maximum energy level that the free electrons can have when the material is at an absolute temperature of zero degrees. The free electrons are distributed in the energy states below the Fermi level from a minimum energy level.

On the other hand, the work function is defined as the energy required to release an electron that is confined within the material. This energy basically overcomes the Coulombian interaction generated by the effect of the image charge in the material due to the absence of the electron.

Taking these two concepts into consideration, when the temperature of a material is raised, it is capable of yielding thermal energy to the electrons; when this is greater than or equal to the work function, the electrons will be free, that is, they will be outside the material. By external factors, energy can be given up to the emitted electrons so that they can move through the vacuum to another material. When two plates of different materials separated by a certain distance are used in which the emitter has a higher work function than the collector, then the electrons that are received in the latter will have a higher energy than the former. This generates a surplus of energy which is translated as electromotive force capable of powering a charge in the system. The potential in the charge is generated by the energy difference in the Fermi levels of the emitter and collector.

Ideally, it is required that the electron flow does not lose energy during its path, however, in practice, energy losses occur in the interelectronic region, as well as when the flow impinges on the collector.

The emission of electrons in the absence of an external electric field is explained by the Richardson-Dushman equation. On the other hand, the behavior of the electron flow in the interelectronic region is obtained from the Langmuir - Child law. This equation determines the current density as a function of the applied electric field and the distance between the electrodes. Furthermore, considering the effect of the applied field on the confining surface potential barrier of the material, it is found that the Schottky equation correctly describes this phenomenon.

Electronic valves and thermionic converters present similar I - V curves that can be explained from their origin to their saturation by means of these equations.

Figure 1 shows a cesium thermionic converter whose emitter and collector are separated by an insulator; the separation distance between the two electrodes is in the order of tenths of a millimeter.

The converter housing is hermetically sealed, so the internal atmosphere can be controlled. In the conventional converter, the interelectrode space is filled with cesium vapor, and the cesium working pressure is of the order of 1 torr.

Cesium, in thermionic converters, performs two basic functions; the first is that it adsorbs on the electrode surfaces to improve their emission capacity, and the second is to generate positive ions on the surface of the emitter with which it is possible to neutralize the electron space charge generated by heating in the space adjacent to the surface of the emitter. The elimination of this space charge and the ease of electron transport make it possible to obtain practical current densities.

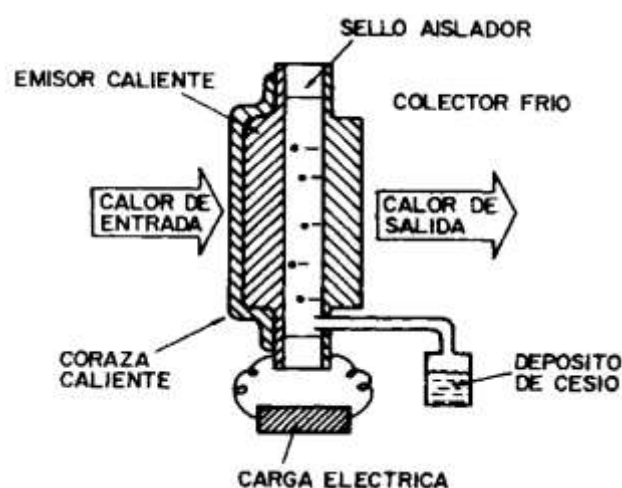


Figure 1 Thermionic converter

The thermionic converter, from the thermodynamic point of view, is a heat engine that uses the electron gas as working fluid, therefore, its efficiency cannot exceed that established by the Carnot cycle. The temperature difference between emitter and collector pulls the electrons through the system charge.

For a given set of electrodes, the output power of the thermionic converter is a function of the collector and emitter temperature, the interelectrode spacing and the pressure of the cesium atmosphere. Usually, thermionic converters operate at high temperature. Typically, the emitter temperature is in the range of 1600 to 2400K, and the collector temperature varies from 800 to 1100K, thus making it possible to obtain current densities ranging from 5 to 10 A/cm² at an output potential of the order of 0.5V. The efficiency of this type of converters to generate electricity from heat varies between 10 and 15%.

The objective of the present work is: to simulate the behavior of the electrons emitted between the electrodes of a thermionic converter, in order to find the emission capacity of a thermionic converter as a function of the parameters involved.

The simulation of the electron flow behavior will show the emission capacity of a thermionic converter, as a function of the main parameters involved.

1. Basic theory of electron emission

It is known that a metal contains a large number of free electrons in its interior, which move easily in the presence of applied electric fields, even if these are of low intensity. However, when the electrons approach the surface, they cannot escape due to the surface confinement potential which can be modified by external factors. The following is a brief review of the theories that have been developed to explain the phenomenon of electron emission in a thermionic converter.

1.1 I - V characteristics of a vacuum thermionic diode

The vacuum diode is an electronic device with two terminals, which are connected to the emitter and collector. The intermediate space between emitter and collector can be vacuum (high vacuum diodes) or cesium plasma (cesium diodes). The emitter is characterized because it emits electrons when it is at a high temperature, when an external voltage is applied between it and the collector, the current flowing through the device behaves according to the curve shown in Figure 1.1, which is typical of an experimental high vacuum thermionic diode.

It can be reproduced from the fundamental equations explaining thermionic emission.

Figure 1.2 (a) shows the electrostatic potential profile between the electrodes of the thermionic diode. Here, $E_F(\varepsilon)$ is the Fermi level of the emitter, $E_F(c)$ that of the collector and ϕE and ϕC their corresponding work functions. V is the voltage

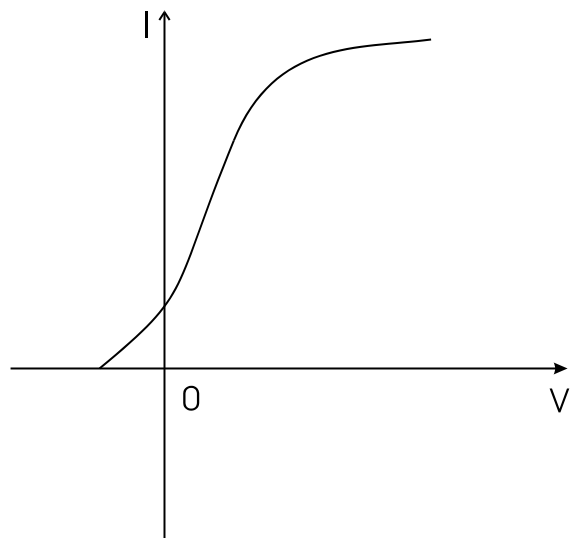


Figure 1.1 Characteristic curve of an experimental thermionic diode

Of charge generated by the energy difference in the Fermi levels. Region (1) denotes the case of the ideal diode model that neglects the space charge effect which generates a potential barrier at the electrode surfaces that substantially affects the transit of the emitted electrons.

This effect is reduced by considering reduced spaces between emitter and collector. Region (2) represents the actual potential profile considering space charge effects. In (b), the thermionic current density versus output voltage is plotted for the ideal (1) and real (2) case of the diode. At V equal to zero is the closed-loop case (3), and at (4) the open-loop case ($J=0$). There are other methods to reduce the space charge effect that are not of interest to study for now. In practice it has not been possible to operate thermionic diodes at spacings smaller than 0.01 mm. For this range of values, the output power density is less than 1.0 W/cm². Using cathodes for the emitter (1538 K) and collector (810 K), G. N. Hatsopoulos obtained a current density of 1.0A/cm² at an output potential of 0.7V.

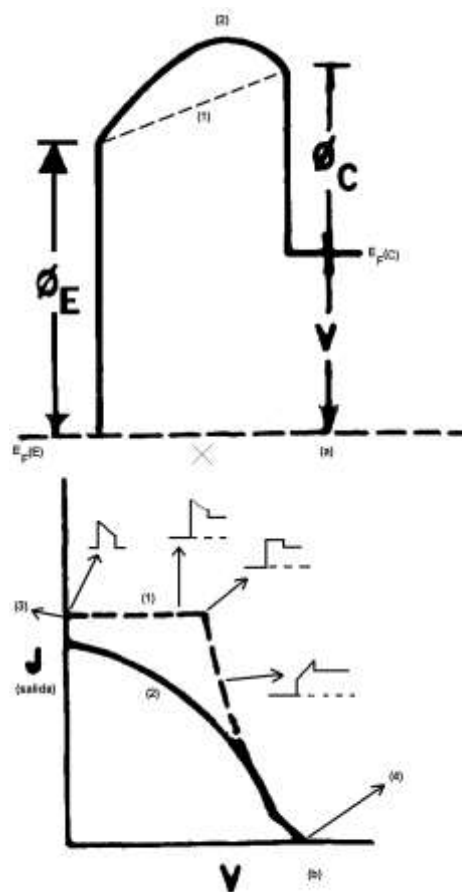


Figure 1.2 (a) Variation of the electrostatic potential profile (b) Thermionic current vs. output voltage

1.2 Description of electron emission on a hot metal surface (Richardson - Dushman Equation)

When the temperature of a metal increases, some of the electrons in the solid gain enough thermal energy to overcome the binding forces to free themselves from the solid, this process is called thermionic emission. As the temperature increases, the number of electrons emitted increases. Thermionic emission depends on the physical parameters of the solid, especially the work function ϕ and the temperature. Figure 1.3 (b) shows the energy distribution of electrons in a solid. When the x-component of the velocity of the electrons impinging on the surface is greater than,

$$v_{xc} = \frac{p_{xc}}{m} = \sqrt{\frac{2(E_F + \phi)}{m}}, \quad (1.1)$$

(where $E_F + \phi$ is the minimum energy required to be released from the solid).

The electrons will overcome the surface forces along the normal to the surface and will be emitted.

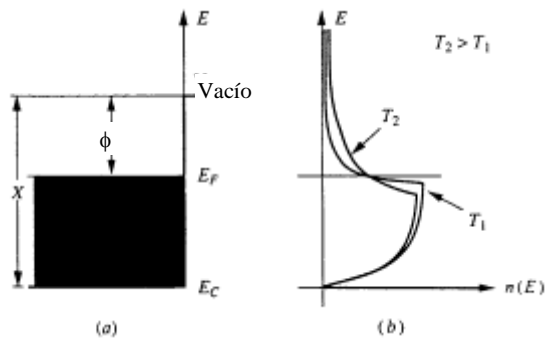


Figure 1.3 (a) Band diagrams of energies and (b) Electron energy distribution in a solid

The current density, thermally emitted in the x-direction is by definition equal to

$$dJ_{th} = ev_x n(v) dv \quad (1.2)$$

With $n(v)$ the electron velocity distribution. The total current density due to the contribution of all electrons is given by

$$J_{th} = \int_{-\infty}^{\infty} \int_{-\infty}^{\infty} \int_{-\infty}^{\infty} \frac{2m^3}{h^3} \frac{v_x dv_x dv_y dv_z}{1 + \exp\left[m(v_x^2 + v_y^2 + v_z^2)/2kT - (E_F/kT)\right]} \quad (1.3)$$

Since the energy required for the electrons to be emitted is greater than E_F , one can disregard the unit in the denominator and write equation (1.3) as

$$J_{th} \approx e \frac{2m^3}{h^3} \exp\left(\frac{E_F}{kT}\right) \int_{v_{x0}}^{\infty} \exp\left(-\frac{mv_x^2}{2kT}\right) v_x dv_x \int_{-\infty}^{\infty} \exp\left(-\frac{mv_y^2}{2kT}\right) dv_y \int_{-\infty}^{\infty} \exp\left(-\frac{mv_z^2}{2kT}\right) dv_z \quad (1.4)$$

Finally, equation (1.4) becomes:

$$J_{th} = \frac{4em\pi k^2 T^2}{h^3} \exp\left(-\frac{\phi}{kT}\right), \quad (1.5)$$

Yes A_0 is defined as:

$$A_0 = \frac{4\pi emk^2}{h^3} = 1.2 \times 10^6 \text{ A/m}^2 \text{K}^2 \\ = 120 \text{ A/cm}^2 \text{K}^2$$

Then J_{th} can be written as:

$$J_{th} = 120 T^2 e^{-\phi/kT} \text{ A/cm}^2 \quad (1.6)$$

Expression 1.6 is known as the Richardson-Dushman equation.

It is observed that, at a given temperature, a solid with a lower work function will emit more electrons than one with a higher one, there is also a strong dependence of the emission current density on temperature.

The constant $A_0 = 1.2 \times 10^6 \text{ A/cm}^2 \text{K}$, in general is different for real solids. The surface forces, the type of emitting material and the surface roughness of the material modify the value of A_0 . The temperature behavior given by equation 1.6 has been verified experimentally in many materials.

1.3 Behavior of electron flow subject to an electric field (Langmuir - Child Eq.)

The analysis of a diode is particularly simple when the cathode and anode are flat, parallel surfaces, with very little separation between them. In the following study, it is assumed that the electric field is perpendicular to the electrodes at all their points (thus neglecting edge scattering). It can be seen that the relationship between the current and the potential to be obtained also describes the behavior of devices whose geometrical shapes are more complex. Figure 1.4 shows schematically the geometrical shape of the diode to be analyzed.

Next, the behavior of electrons subjected to an external electric field is examined. Consider the cathode at a temperature T , such that there is an appreciable emission of electrons generating a charge density in the interelectronic space. The equation relating the electron density to the potential at any point in the interelectronic space is Poisson's equation,

$$\frac{d^2V}{dx^2} = -\frac{\rho}{\epsilon_0} \quad (1.7)$$

Where V satisfies that at $x=0$, $V(0)=0$ and at $x=d$, $V(d)=V_a$.

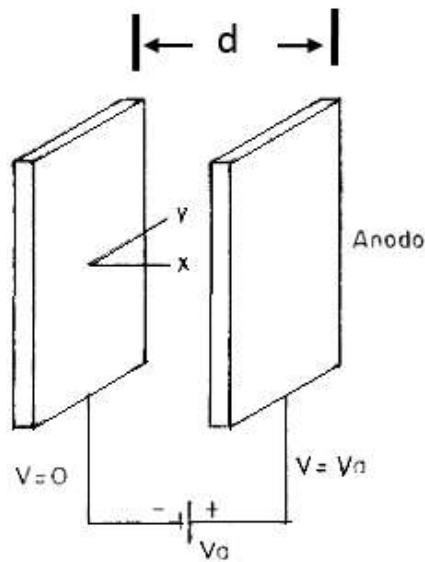


Figure 1.4 Potentials and geometrical aspects of the diode

To find a relationship between the current density flowing between cathode and anode, with the applied potential and the separation distance d , the basic relationship is evoked,

$$J = -Nev = -\rho v \quad (1.8)$$

On the other hand, at any point in the interelectronic space is satisfied:

$$eV(x) = \frac{1}{2}m[v(x)]^2 \quad (1.9)$$

Where $V(x)$ is the potential and $v(x)$ is the velocity. From equations (1.7), (1.8) and (1.9) we obtain

$$\frac{d^2V(x)}{dx^2} = \frac{-JV(x)^{-1/2}}{\left(2\frac{e}{m}\right)^{1/2}\epsilon_0} \quad (1.10)$$

Solving equation 1.10 for the current density J , it follows that:

$$J = 2.33 \times 10^{-6} \frac{V_a^{3/2}}{d^2} \quad (1.11)$$

Note that equation 1.11 depends only on the applied potential and the separation distance, ignoring the cathode temperature and work function. This result is known as the Langmuir - Child law or three-medium power law.

In practice, the current density values may be lower than those predicted by equation (1.11) because the electron emission at the cathode is limited by the cathode temperature mainly when the cathode temperature is low.

1.4 Schottky effect

The derivation of the thermionic emission equation is based only on the electrons that overcome the work function of the solid due to the thermal energy they have associated with them at a given temperature T . Some of the electrons that become free are forced out of the cathode and towards the anode by the application of an external potential between these two electrodes. At low potentials the characteristic electron emission does not change, but at high potentials, i.e. high electric fields, the current density by thermionic emission from the cathode changes significantly. This phenomenon is known as the Schottky effect.

The idealized potential barrier seen by an electron in the solid is shown by the dotted line in Figure 1.5.

When the electrons are free they move a distance x away from the solid generating a positive charge on the solid (image charge effect). The resulting Coulomb force between these two charges separated by a distance of $2x$ is

$$F_x = -\frac{e^2}{4\pi\epsilon_0(2x)^2} \quad (1.12)$$

and the associated potential energy is:

$$\Phi_s(x) = -\frac{e^2}{16\pi\epsilon_0 x} \quad (1.13)$$

If an external electric field directed towards the surface of the emitter is now considered, then the electron experiences an additional potential due to this applied field ϵ . The resulting potential at a distance x away from the surface is

$$\Phi_e(x) = -e\epsilon x \quad (1.14)$$

The externally applied field effectively reduces the equivalent potential barrier for the electron in the solid as shown in Figure 1.4.

The total potential energy is

$$\Phi_t(x) = \Phi_e(x) + \Phi_s(x) \tag{1.15}$$

The effect of the external field reduces the work function W to a value $W' < W$. The thermally emitted electrons now experience an equivalent work function W' , this results in a current density given by:

$$J_e = A_o T^2 e^{-W'/kT} \tag{1.16}$$

Which in terms of the electric field is written as:

$$J_e = J_{th} \exp\left[\frac{e(e\mathcal{E} / 4\pi \epsilon_o)^{1/2}}{kT}\right] \tag{1.17}$$

The externally applied electric field then increases the density of the emitted electrons.

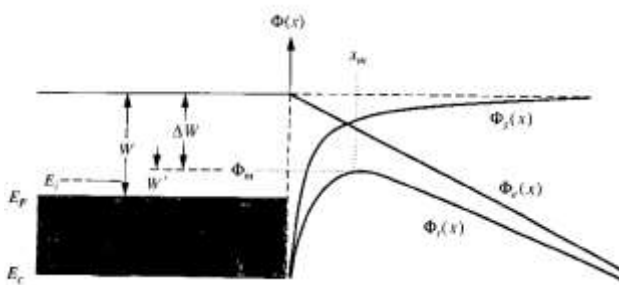


Figure 1.5 Modification of the idealized potential barrier (dashed line) for a solid with image potential $\phi_e(x)$ and additional potential $\phi_s(x)$ due to the applied external electric field

1.5 Hatsopoulos' Ideal Diode Model

The ideal model of a thermionic converter corresponds to a diode in which the emitter and collector are placed very close to each other. In order to reduce the complexity of the equations, the effects due to ion emission are also neglected. Although these assumptions do not strictly correspond to some thermionic converter, they approximate a close-spaced diode operating in the vacuum mode. The ideal diode model defines the limit of the development that can be expected for a thermionic converter and provides a basis for comparison of practical converters.

In the Hatsopoulos model, the current density J across the load was considered to consist of JEC flowing from the emitter to the collector minus Jce flowing from the collector to the emitter, thus

$$J = AT_E^2 \exp\left(-\frac{V + \phi_c}{KT_E}\right) - AT_C^2 \exp\left(-\frac{\phi_c}{KT_C}\right) \tag{1.18}$$

For $V + \phi_c > \phi_E$ and V voltage at the output load.

When the output voltage is reduced such that: $V + \phi_c < \phi_E$ then:

$$J = AT_E^2 \exp\left(-\frac{\phi_E}{KT_E}\right) - AT_C^2 \exp\left(-\frac{\phi_E - V}{KT_C}\right) \tag{1.19}$$

Equations (1.17) and (1.18) can be used for the construction of the $J - V$ curve, for different values of ϕ_e , ϕ_c , T_e and T_c . Usually $1600 < T_e < 2000K$, $600 < T_c < 1200K$, $2.4 < \phi_e < 2.8eV$ and $\phi_c \cong 1.6 eV$

Thermionic electric power production. It exploits the difference in the electron fluxes of the two surfaces facing each other at different temperatures, thus the net current is stable. Figure 1.6 shows a cell with the electrodes facing each other at different temperatures. The electrode at the higher temperature generally emits a higher current than the cold electrode, so a net current is obtained.

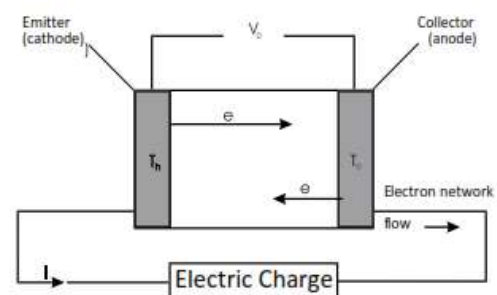


Figure 1.6 The thermionic diode as an energy converter

2. Description of the algorithms used for the theoretical study of natural and forced emission

The mathematical algorithm used to determine the thermionic emission, by means of the Richardson - Dushman equation, is described by means of flow diagrams; for this, the temperature is varied while the work function is kept constant. To calculate the thermionic emission between two electrodes separated by a constant distance, the equation developed by Hatsopoulos for the vacuum diode is used. The forced emission or field emission is calculated from the Langmuir - Child equation. Finally, the algorithm to evaluate the high field emission (Schottky effect) is developed.

2.1 Algorithm to determine the current density for different temperatures in the emitter

The behavior of the current density generated for different temperatures in the emitter of a thermionic diode while keeping the work function of the material fixed is determined by the Richardson - Dushman equation, *i.e.*:

$$J_{th} = A_o T^2 \exp\left(-\frac{\phi}{kT}\right) \quad \frac{A}{m^2} \quad (1.6)$$

$$A_o = 1.2 \times 10^6 \quad \frac{A}{m^2 K^2}$$

With

And further where:

k = Boltzmann's constant

ϕ = Work function

T = Absolute temperature (K)

To calculate the electron emission at a hot electrode by means of the Richardson - Dushman equation for different work functions, the evaluation algorithm was first defined by means of the flow diagram in Figure 2.1.

In the first block, the Richardson - Dushman equation is introduced to the plot, and then the value of the work function is chosen for different values between 2.0 and 5.5, with increments of 0.5 eV. In the next block, the evaluation of the equation for temperature variations between 0 and 4000K is done to obtain the corresponding graph.

If it is desired to obtain another graph for another work function, it is returned to the point where this one is chosen. Once the evaluations of the different graphs are finished, the process is printed and the process is finished.

2.2 Algorithm to determine the behavior of the electron flow in a thermionic diode

If a vacuum thermionic converter has emission and collection surfaces with dimensions much larger than the interelectronic space d , the net electron flow in the interelectronic space is almost unidirectional. Therefore, the output current characteristic can be presented in terms of the output current density. If the reverse emission current density is not negligible, then:

$$J = AT_E^2 \exp\left(-\frac{\phi_E}{kT_E}\right) - AT_C^2 \exp\left(-\frac{\phi_C}{kT_C}\right) \quad (1.19)$$

Where:

ϕ_E = Work function at emitter.

ϕ_C = Work function at the collector

TE = Emitter temperature

TC = collector temperature

k = Boltzmann constant

To evaluate the behavior of the electron flow in a thermionic diode according to the mathematical model proposed by Hatsopoulos, the sequence defined by flow diagrams 2.2 and 2.3 was used.

Flowchart 2.2 operates as follows; first the equation of the ideal diode model proposed by Hatsopoulos is introduced, then a work function between 2.4 eV and 4.0 eV with increments of 0.4 eV is chosen. The equation is then evaluated by varying the emitter temperature between 1000 and 3000K. For each evaluation developed, the emitter temperature was considered equal to 800 K and its work function equal to 3 eV. If it is desired to obtain another graph for another work function, it is returned to the point where this one is chosen, after evaluating the emission for different work functions, the graph is printed and the process is finished. The flow chart in Figure 2.3 was developed to evaluate the emission of the ideal diode when the collector temperature is varied. For this, the emitter conditions are first defined and then a work function is chosen for the collector between 1 and 1.8 eV with 0.2 eV increments. The collector temperature is varied in the range between 300 K and 2000K.

If it is desired to obtain another graph for another work function, it is returned to the point where this one is chosen, finally, the graph is printed and the process is finished.

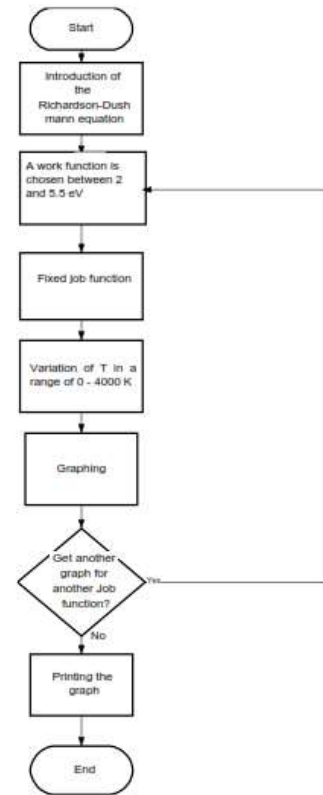


Figure 2.1 Flow chart for calculating electron emission by means of the Richardson - Dushman equation

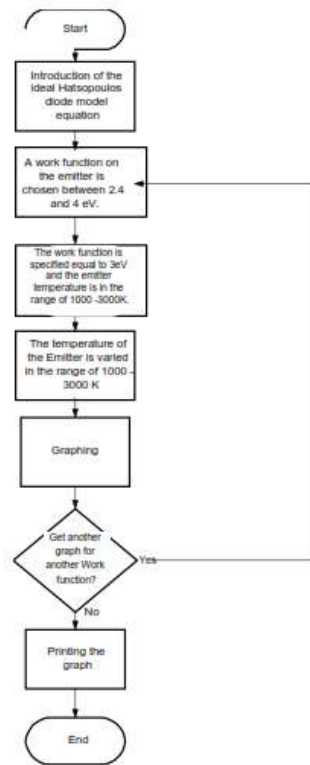


Figure 2.2 Flow chart to calculate the electron emission in a thermionic diode when the temperature of the emitter is varied

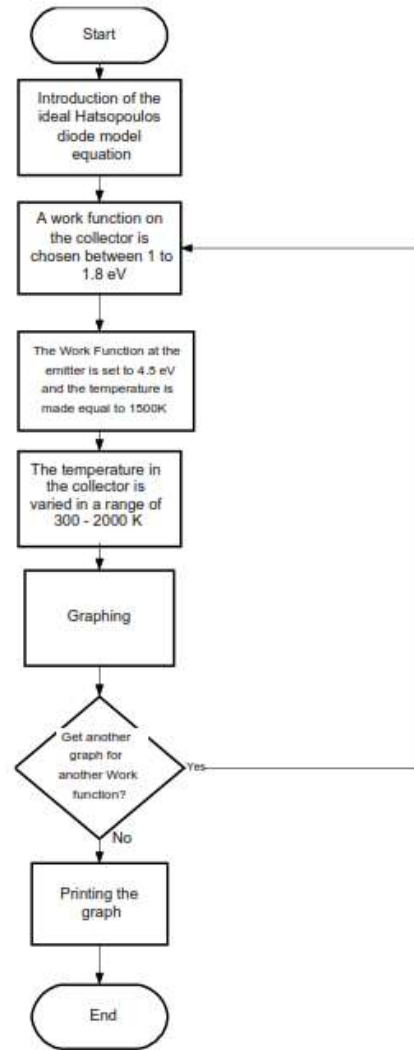


Figure 2.3 Flow chart to calculate the electron emission in a thermionic diode when the collector temperature is varied

2.3 Algorithm to determine the electron flow behavior for field variations

The behavior of the current density when a potential is applied to the anode and there is a distance d between the electrodes is determined by the Langmuir - Child equation.

$$J = 2.33 \times 10^{-6} \frac{V_a^{3/2}}{d^2} \tag{1.11}$$

Where:

J = Is the current density between the electrodes, in A/m².

V_a = Voltage applied between the plates, in Volts.

d = is the separation distance between the electrodes, in meters.

In the algorithm shown in Figure 2.4 the Langmuir - Child equation is first introduced and then evaluated for different interelectronic separation distances.

The values chosen for these distances are: 0.01, 0.02, 0.05, 0.1, 0.5 and 1 μm . After a distance is chosen, the electric field is varied in the range of 0 to 0.016 V/ μm . If you want to obtain another graph for another distance, go back to the point where this one was chosen, when the sequence is finished, print the graphs and end the process.

2.4 Algorithm to determine the current density for field variation while the emitter temperature is kept constant

To calculate the current density for electric field variations when the emitter temperature is kept constant, the emitting electrode is brought to saturation, and the Langmuir - Child and Richardson - Dushman law equations are combined, for this the algorithm shown by the flow chart in Figure 2.5 was defined. First, the Langmuir - Child equation is introduced and calculated for an interelectronic distance of 0.1 mm. Subsequently, the electric field is varied in the range of 0 to 0.16 V/mm. On the other hand, to determine the saturation current of the emitter, it is evaluated with the Richardson - Dushman equation for a work function of 4.5 eV. Emitter temperatures of 2700, 2800, 2900, 3000, 3100 and 3200 K were chosen. Finally, the obtained results were combined and the process is finished with the printing.

2.5 Algorithm to evaluate the behavior of the electron flow due to the Schottky effect

The behavior of the current density for different temperatures, while keeping the work function of the emitter fixed, is determined by the Schottky equation, ie:

$$J_e = J_{th} \exp\left[\frac{e(e\mathcal{E} / 4\pi \epsilon_0)^{1/2}}{kT}\right] \quad (1.17)$$

Where

J_{th} = Richardson - Dushman Equation

e = Electron charge (C)

\mathcal{E} = Electric field (V/m)

ϵ_0 = Permittivity in vacuum (C²/Nm²)

k = Boltzmann constant

T = Absolute temperature (K)

To calculate the current density when an electric field is applied, at a fixed temperature and constant work function at the emitting electrode, the Schottky equation is used, the algorithm defined to perform these calculations is shown in Figure 2.6.

In the first block, the Schottky equation is introduced and then a value is chosen for the emitter temperature in the range of 800 to 1500 K with 100 K increments. In the next step, the electric field in the range 0 to 1E6 V/m is varied. If another graph is desired, for another temperature, return to the point where a new temperature is chosen. Finally, the graphs are printed and the process is finished.

Algorithm to determine the I vs V behavior of an ideal thermionic converter.

To determine the current with respect to voltage in an ideal thermionic converter, the emission current equation 2.11 is used.

$$J = AT_E^2 \exp\left(-\frac{\phi_E}{kT_E}\right) - AT_C^2 \exp\left(-\frac{\phi_C}{kT_C}\right) \quad (1.19)$$

and $\phi_E = \phi_C + eV$

Where:

ϕ_E = Emitter work function.

ϕ_C = Work function at the collector

T_E = Emitter temperature

T_C = collector temperature

k = Boltzmann constant

V = Voltage at the load

To calculate the current, the flow diagram in Figure 2.7 was used for different emitter work functions in the range of 1.8 eV to 5 eV. In this case, the emitter work function is substituted by the sum of the collector work function and the load voltage. In this way, the behavior of the emitter current can be determined for values of expected load voltage even larger than its own work function. This adequacy of the equation simulates the fraction of electrons generated with higher kinetic energy than specified by the work function.

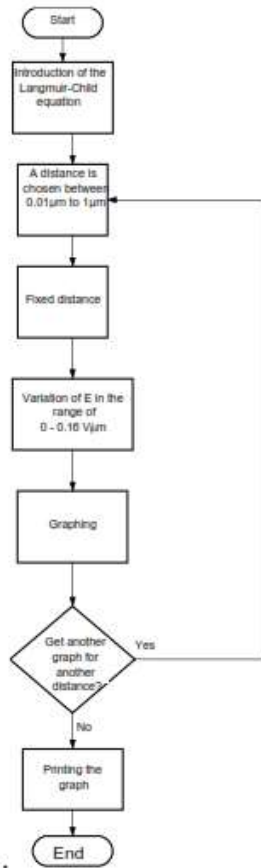


Figure 2.4 Flow diagram to determine the electron flow behavior according to the Langmuir - Child law.

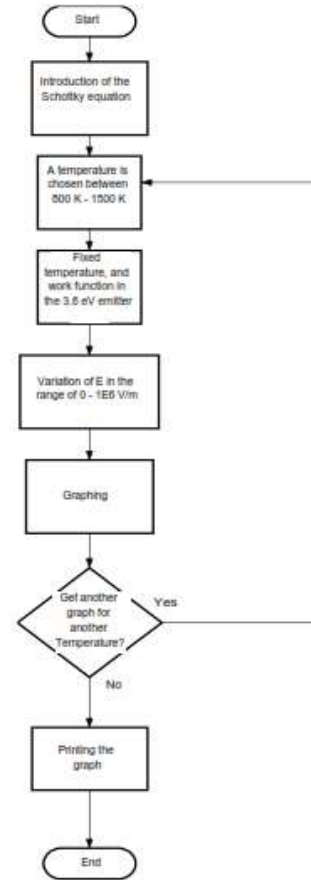


Figure 2.6 Flow diagram to determine the behavior of the electron flow due to the Schottky effect

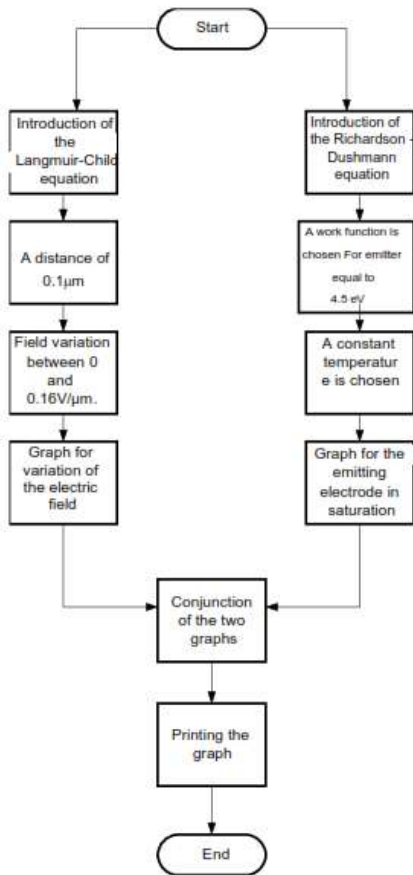


Figure 2.5 Flow diagram to determine the electron flow behavior by combining the Langmuir - Child and Richardson - Dushman equations

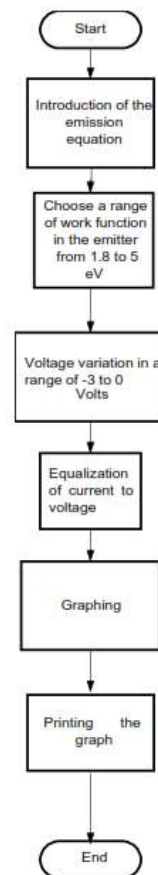


Figure 2.7 Flow chart to determine the behavior of an ideal diode using equation 1.11 developed by Hatsopoulos

3. Results and discussion

The graphical behavior of the current density for a thermionic diode when it operates naturally and when an external electric field is applied to it is shown below. Several exercises are shown for different work functions and temperature variations. The expected result for a thermionic diode with predefined characteristics is also shown.

3.1 Emitter current density behavior of a thermionic diode for different temperatures.

To determine the behavior of the current density generated for different temperatures, the temperature in the emitter was considered in a range from 300 to 3000 K, for a variation of the work function of the emitter from 2.5 to 5 eV with increments of 0.5 eV; with these conditions the behavior of the current density for different temperatures in the emitter was found as shown in Figure 3.1.

It can be seen in this Figure 3.1, that the onset of electron emission at the electrode requires a higher temperature for a high work function than for a low function.

For a work function of 2.0 eV, appreciable emission starts at around 1250 K.

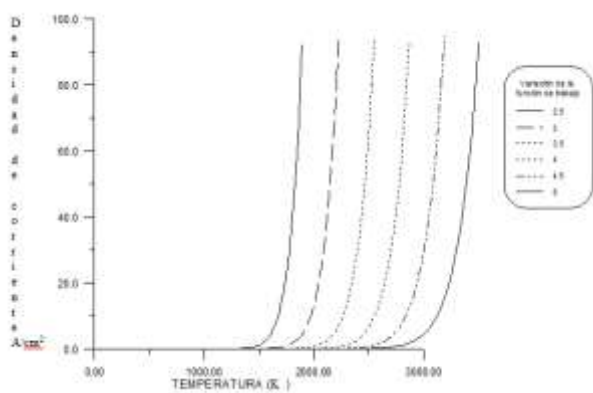


Figure 3.1 Behavior of current density at the emitting electrode as a function of temperature for different work functions

3.2 Vacuum thermionic converter

To determine the behavior of the current density in a vacuum diode, the following conditions were proposed:

T variations in the range of 1000 to 3000K, work functions at the emitter between 2.4 and 4 eV, constant collector temperature of 800K and constant collector work function equal to 2 eV.

Figure 3.2 shows the characteristics of the current density for different work functions in the emitter, it can be seen that for a lower work function a higher current density is reached for the same temperature.

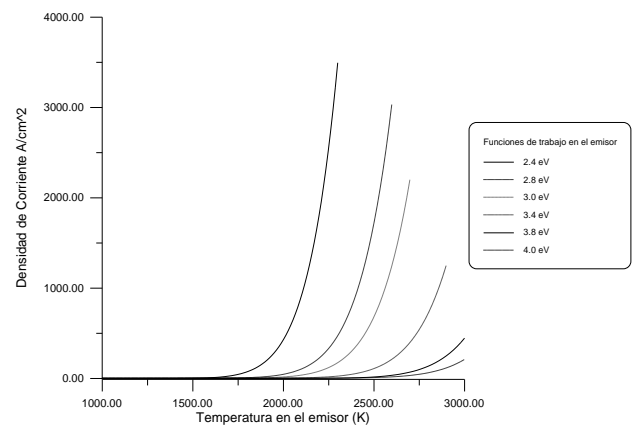


Figure 3.2 Current density behavior in a vacuum diode for temperature variations in the emitter and different work functions of the same

Figure 3.3 shows the current density for Tc variations between 300 and 1200K, collector work functions between 1 and 1.8eV at a constant emitter temperature equal to 1500K, and constant emitter work function equal to 2.5 eV. Figure 3.3 also shows the variation of the current density for different work functions at the collector, in this case, the inversion of the current in the diode is observed from 700K. The inversion of the current density is not appreciable for collector work functions higher than 1.4 eV.

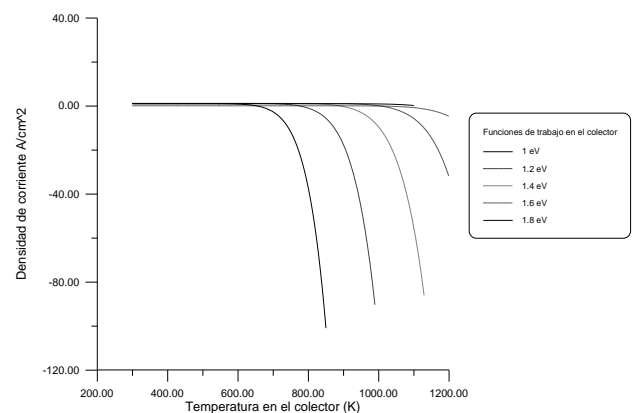


Figure 3.3 Current density behavior in a vacuum diode for temperature variations in the collector and different work functions of the diode

Behavior of the current density in a thermionic diode for field variation.

To determine the behavior of the current density generated for different temperatures, the following parameters were considered: the electric field was varied in a range from 0 to 0.16 V/m, varying the interelectronic distance from 0.01 to 1mm obtaining Figure 3.4.

Figure 3.4 shows the characteristics of the current density generated when the electric field is varied while the interelectronic distance is kept constant. It can be seen that, at greater distances, a more intense electric field is needed to obtain a current density equivalent to the density obtained for smaller distances.

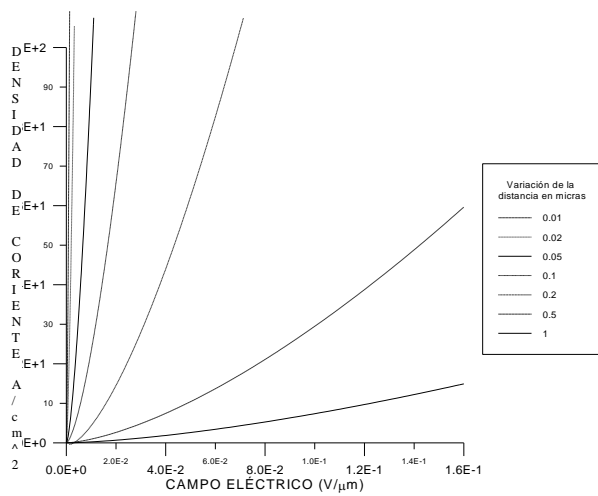


Figure 3.4 Expected behavior of the current density in a thermionic diode when the field is varied while the emitter temperature is kept constant

As can be seen from the graph in Figure 3.5, a conjunction of the two electronic emission equations leads the emitting electrode to saturation. The behavior of the increasing current density is given by the Langmuir - Child equation, and saturation is established by the Richardson - Dushman equation. The independent variable is the electric field.

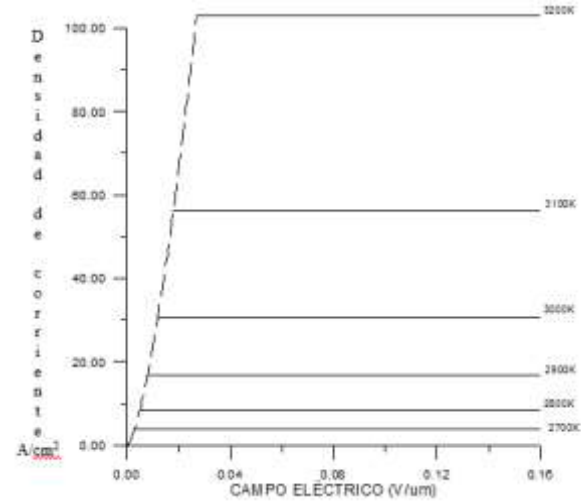


Figure 3.5 Current density behavior with respect to field variation for different temperatures. The interelectronic separation was kept constant and equal to 0.1um, the work function in the emitter was made equal to 4.5 eV

3.5 Current density behavior in a thermionic diode for field variation according to Schottky's equation

In the behavior of the current density for the thermionic diode according to the Schottky equation, an electric field in a range from 0 to 1.6E6 V/m is considered, being parametric in the temperature in the range from 1000 to 3000 K in the emitter, with increments of 500K, maintaining a work function in the same of 4.5 eV. Figure 3.6 shows the current density characteristics for different temperatures, when varying the electric field and constant work function at the emitter.

It can be seen that for the different temperature conditions, the electric field generates a further increase of the current density in contrast to the saturation point calculated with the Richardson - Dushman equation. This can be seen as a modulation of the saturation point generated by the external electric field.

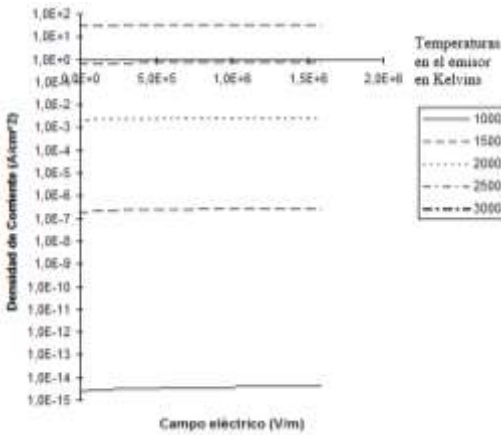


Figure 3.6 Behavior of the current density emitted by an emitter electrode for field variations. The work function of the emitter remains constant and equal to 4.5 eV.

3.6 I vs. V behavior of an ideal thermionic converter

To determine the expected current vs. voltage behavior of an ideal thermionic converter, a particular case was proposed. In this example, the work function at the emitter is assumed to be 2.8 eV, the collector work function is assumed to be 1.8 eV, the emitter temperature is assumed to be 1364 K, the collector temperature is assumed to be 600K, and an emission area at the emitter is assumed to be 2 cm².

As seen in the graph of Figure 3.7; the ideal diode has a growth with respect to the voltage, which starts at -1.8V and ends at the 20 mA point.

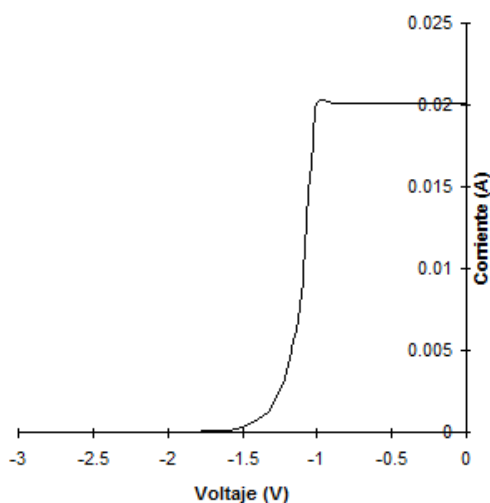


Figure 4.7 Comportamiento de la corriente generada por un convertidor termoiónico ideal; para funciones de trabajo en el emisor y colector de 2.8 eV, 1.8 eV. Respectivamente, la temperatura en el emisor es de 1364K y en el colector es de 600 K, además, el área efectiva de emisión es de 2 cm²

3.7 I vs. V behavior of a thermionic converter

To determine the expected current vs. voltage behavior of a thermionic converter, a particular case was proposed. In this example it is assumed that the emitter work function is 2.8 eV, the collector work function is equal to 1.8 eV. The interelectronic distance is 0.8 mm. The emitter temperature is 1364 K, and the collector temperature is considered to be 600 K, the emission area is 2 cm².

In the graph of Figure 3.8, a conjunction of the electronic emission equations defines the expected behavior of the current as a function of voltage for the proposed thermionic converter. The starting point corresponds to the open-circuit condition developed by Hatsopoulos. The initial growth of the current is given by the Langmuir - Child equation, and reaching the point of intersection with the electric field equation the Schottky equation begins to predominate. The flat behavior corresponds to the saturation of the diode and the slight lifting of the curve is due to the applied external electric field. Note that when the electric field is zero, the magnitude of the current coincides with the saturation current defined by the Richardson - Dushman equation. Figure 3.8 also shows the ideal behavior of the thermionic converter and the expected behavior when all emission conditions are considered.

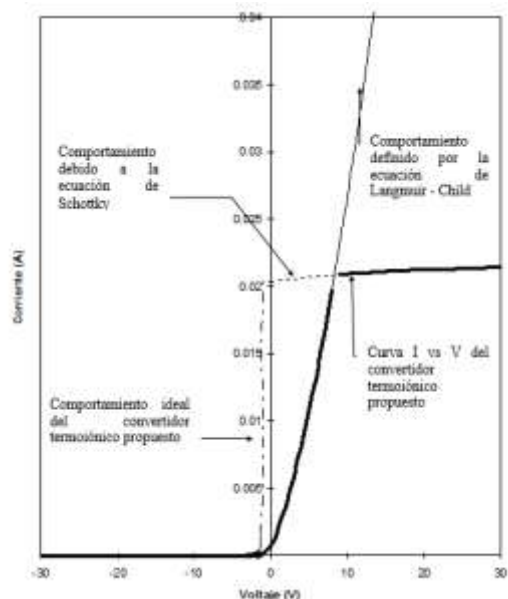


Figure 3.8 Superposition of the curves defined by the Langmuir - Child and Schottky equations for the particular case of a thermionic converter. In this example; $\phi_e = 2.8$ eV, $\phi_c = 1.8$ eV, the interelectronic distance is 0.8 mm, the temperature in the emitter is equal to 1364 K, and in the collector is 600K.

Conclusions

As main conclusions of this work, the following were obtained:

The theory that has been developed to explain electron emission between the electrodes of a thermionic converter was compiled and organized.

The algorithms that allow the use of the equations that predominantly explain the electron emission were developed.

The theory was organized in such a way that the behavior of the current density of a thermionic diode could be obtained independently as a function of: the work function, the temperature, the electric field and the interelectronic separation.

Practical cases related to the expected electronic emission for a thermionic converter were evaluated.

The importance of having low work functions in both the collector and the emitter, in order to work at low temperatures, was observed.

Interelectronic separation is a critical parameter to obtain high current densities.

It was feasible to simulate the behavior of a thermionic diode subjected to an electric field, from the birth of the curve to saturation.

A possible application of this work is to study the behavior of electron emission in nanometer thermionic structures. This study can be used to develop close-spaced thermionic converters, and also to study high-field emission; the latter can be useful for the development of high-vacuum microelectronics.

References

S.W. Angrist, (1982) *Direct Energy Conversion*, Boston Allyn and Bacon Inc.

G.N. Hatsopoulos, (1956), *The Thermoelectron Engine*, M. I. T: (Sc. D. Dissertation)

G.N. Hatsopoulos, E.P. Gyftopoulos, (1978) *Thermionic Energy Conversion*, Vol I: Theory, Technology, and Application Massachusetts: MIT Press, Cambridge.

C.I., Hemenway, R.W. Henry, M.Coulton (1983), *Física Electrónica*, México: Limusa, Noriega Editores.

A.M. Ferendeci, (1991), *Physical Foundations of Solid State and Electron Device*, New York: Mc. Graw-Hill, Inc.

J. Millman, S. Seely, (1951), *Electronics*, Mc. Graw-Hill Second edition.

R. Decher, (1977) *Direct Energy Conversion (Fundamentals of electric power production)*, Oxford: University Press,

A, Dimarco (1962), *Electronica*, Argentina: El ateneo.

Wilson, V. C. (1959). Conversion of heat to electricity by thermionic emission. *Journal of applied physics*, 30(4), 475–481. <https://doi.org/10.1063/1.1702391>

Liang, S.-J., & Ang, L. K. (2015). Electron Thermionic Emission from Graphene and a Thermionic Energy Converter. *Physical Review Applied*,3(1). <https://doi.org/10.1103/physrevapplied.3.014002>

Zhao, M., Fang, S., Jiang, Z., & Yu, J. (2023). Mathematical model establishment and optimum design of a novel cesium thermionic–thermoelectric hybrid generator. *Applied Thermal Engineering*, 120995, 120995. <https://doi.org/10.1016/j.applthermaleng.2023.120995>

Integrative project: CNC technology and micro-wire (MIG) welding for precision and efficiency in industry

Proyecto integrador: Tecnología CNC y soldadura de microalambre (MIG) para la precisión y eficiencia en la industria

ZUNIGA-MORENO, Juan[†]*, COTERO-RODRÍGUEZ, Arelly Eunice and MORALES HERNÁNDEZ, Victor

Universidad Tecnológica Cadereyta

ID 1st Author: *Juan, Zuñiga-Moreno* / ORC ID: 0009-0007-3158313X, CVU CONAHCYT ID: 1104128

ID 1st Co-author: *Arelly Eunice, Cotero-Rodríguez* / ORC ID: 0009-0006-8335-4438, CVU CONAHCYT ID: 632963

ID 2nd Co-author: *Víctor, Morales-Hernández* / CVU CONAHCYT ID: 1306323

DOI: 10.35429/JTO.2023.19.7.31.36

Received March 10, 2023, Accepted, June 30, 2023

Abstract

In this scientific divulgation article, the impact of Computer Numerical Control (CNC) welding machines in the welding industry will be explored through an integrative project carried out at the Universidad Tecnológica Cadereyta. The main objective is to analyze the importance and added value of this technology in terms of control and automation of welding processes, as well as the power plant that supports its implementation and the safety of the developed prototype. In this sense, the significance of the variables involved in the project will be discussed and the criteria used for their evaluation will be compared. In addition, an overview of the results obtained and the conclusions derived from this project will be shared. Also, possible areas for improvement in this field will be highlighted, considering future research opportunities. In summary, this popular science article examines the impact of CNC welding machines in the welding industry, highlighting their importance, the problems they address and the relevance of safety in their implementation. In addition, it presents the results obtained, the conclusions of the project and the prospects for future improvement.

Welding, Industry, Technology

Resumen

En este artículo de divulgación científica, se explorará el impacto de las máquinas soldadoras de Control Numérico por Computadora (CNC) en la industria de la soldadura a través de un proyecto integrador llevado a cabo en la Universidad Tecnológica Cadereyta. El objetivo principal es analizar la importancia y el valor añadido de esta tecnología en términos de control y automatización de los procesos de soldadura, así como la central que respalda su implementación y la seguridad del prototipo desarrollado. En este sentido, se discutirá el significado de las variables involucradas en el proyecto y se compararán los criterios utilizados para su evaluación. Además, se compartirá una visión general de los resultados obtenidos y las conclusiones derivadas de este proyecto. Asimismo, se destacarán las posibles áreas de mejora en este campo, considerando las oportunidades de investigación futuras. En resumen, este artículo de divulgación científica examina el impacto de las máquinas soldadoras CNC en la industria de la soldadura, resaltando su importancia, los problemas que aborda y la relevancia de la seguridad en su implementación. Además, presenta los resultados obtenidos, las conclusiones del proyecto y las perspectivas de mejora para el futuro.

Soldadura, Industrial, Tecnología

Citation: ZUNIGA-MORENO, Juan, COTERO-RODRÍGUEZ, Arelly Eunice and MORALES HERNÁNDEZ, Victor. Integrative project: CNC technology and micro-wire (MIG) welding for precision and efficiency in industry. Journal of Technological Operations. 2023. 7-19: 31-36

[†] Researcher contributing as first author.

Introduction

In the field of welding, precision and efficiency are crucial aspects to ensure quality and productivity in manufacturing processes. With the aim of improving these aspects, a project has been developed that seeks to reduce the working time in the welding process and increase accuracy by implementing a CNC (Computer Numerical Control) welding machine prototype.

The overall purpose of this project is to design and implement an efficient and safe prototype for the operator, using computer numerical control to control and monitor the movements of the prototype. This automated approach will provide greater accuracy compared to manually operated machines, resulting in improved surface finish on the parts, reduced production time, reduced operator effort, increased speed and productivity, as well as greater adaptability and safety.

The methodology used in this project is based on a sequence of ordered and proven steps, known as cascade methodology. This methodology has been divided into six staggered steps to facilitate the development of the project.

The first stage of the project focuses on the design of the prototype CNC welding machine. During this stage, a thorough analysis of the operation of the X, Y and Z axes is carried out, and a lightweight structure of considerable size and high speed is developed. The design is carried out using SolidWorks software, which provides a three-dimensional perspective of the machine and facilitates the visualization and modification of components.

The next stage is the selection of materials and components required for the construction of the prototype. Suitable materials are selected for the structure, including supports, guides, bearings and PTR tubes, which allow the joining of all the elements of the base and the creation of the mobile mechanism.

The programming of the prototype is carried out using the MACH-3 software, which allows the machine to be operated both manually and automatically through the G language. This programming allows to control and coordinate the movements of the CNC welder in a precise and efficient way.

Once these initial stages are completed, tests are performed to verify the movements, the operating limits and the calibration of the distance between the torch and the mold. These tests allow the speed and operation of the axes to be adjusted, as well as adjustments to the TB6600 controllers to control the speed of the welder. In terms of the results obtained so far, the first stage of the project, which focuses on the development of the prototype CNC welder, has been satisfactory. The prototype meets the intended performance and represents a significant advance in terms of accuracy and efficiency compared to manually operated machines. However, certain inconveniences have arisen during the process, such as mechanical vibrations, temperature increase and the presence of noise, which required additional adjustments.

Development of Sections and Subsequently Numbered Sections of the Article

First, a thorough investigation of the CNC welding machines available on the market is carried out and their characteristics, advantages and disadvantages are analyzed. Information is gathered on the operating principles of CNC welding machines and the necessary requirements for the design and construction of the prototype are identified. This research helps to establish a solid foundation for the development of the project.

Conceptual design:

Based on the established requirements, a conceptual design of the CNC welder prototype is carried out. Computer-aided design (CAD) software is used to create a three-dimensional representation of the proposed design. During this stage, special attention is given to the integration of key components such as motors, controllers and mechanical structures.

Selection of materials and components

Once the conceptual design is finalized, a careful selection of materials and components to be used in the construction of the prototype is made durable, heat resistant and high quality materials are sought to ensure optimum performance of the prototype. Different component options, such as bearings, guides and fasteners, are also evaluated, taking into account factors such as availability and cost.

Development of the control software

The next step is the development of the control software for the CNC welding machine prototype. Suitable software is selected that allows programming the axis movements and welding operations accurately and efficiently. The G programming language used in CNC machines is learned and the necessary code is written to control the movements and welding operations.

Prototype construction

Once the materials and components have been selected, the CNC welding machine prototype is built. The different parts are assembled according to the conceptual design and the motors, controllers and control software are integrated into the system. During this stage, special attention is paid to the correct installation and connection of the components, as well as the initial calibration of the operating parameters.

Testing and adjustments

Once the prototype is built, extensive testing is performed to evaluate its operation and performance. The precision and smoothness of the axis movements are verified, as well as the quality of the welds made. Adjustments and improvements are made according to the results obtained in the tests, with the objective of optimizing the performance of the prototype and guaranteeing high quality welding results.

Optimization and refinement

Based on the test results and adjustments made, an optimization and refinement stage is carried out. The data collected is analyzed in detail and fine adjustments are made to improve the performance of the prototype. Optimal configurations are sought to maximize the efficiency of the CNC welder.

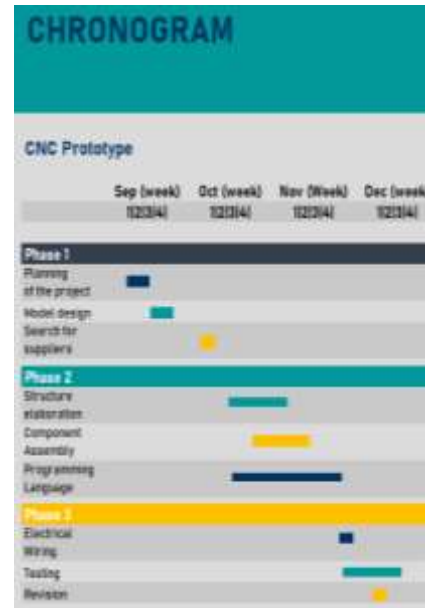


Figure 1 Schedule of activities
Own source without attribution required



Figure 2 Control panel
Source Mach 3 Software

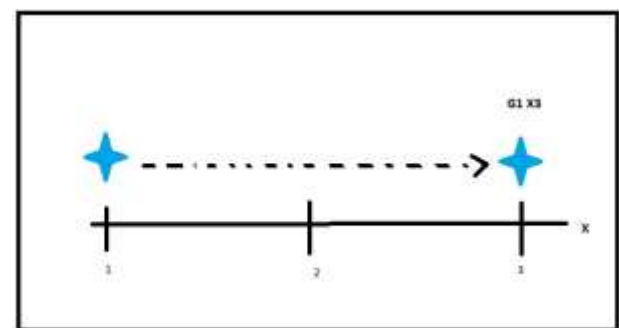


Figure 3 G-coded displacement
Own source without attribution required

Check List CNC Welding Machine				
#	Inspection point	Yes	No	Remarks
1	General cleaning of the machine (5s)			
2	Lubrication of shaft support			
3	Loose or torn cables			
4	Emergency stop Runs			
5	Placement of grounding clamp			
6	Operation of X-axis			
7	Operation of Y-axis			
8	Operation of Z-axis			
9	Operation of X- axis operation (fourth)			
10	Voltage and Amperage Adjustment Control			
11	Limit switch sensor operation			
12	Vibration free			
13	Noise free			
14	Gas Extraction			
15	Power wiring in good condition			
16	Check of torch free of burrs			
17	Motor overheating during the process			

Table 1 Initial inspection table

Source: Own table without required attribution

Methodology to be developed

In the project, the objectives were clearly established and consisted of designing and developing a prototype that integrates mechanical movements and micro wire welding. The success criteria and technical requirements necessary to meet the project expectations were determined.

Extensive research was conducted to become familiar with the fundamental concepts and principles of micro wire welding and mechanical motion systems. Information was gathered on available technologies, required materials and components, as well as best practices in the implementation of similar systems.

Based on the preliminary research, a conceptual design of the prototype was developed, considering aspects such as the mechanical structure, the movement axes, the welding machine and the required electronics. Team meetings were held and design iterations were carried out until a solid and viable proposal was obtained.

Materials and components needed for the construction of the prototype were identified. A shopping list was made and the required elements were purchased, making sure to obtain required elements, making sure to obtain quality products that complied with the established technical specifications.

The assembly and construction of the prototype was carried out following the conceptual design. The displacement axes were assembled, the welding machine was integrated and the necessary electronic elements were connected. Partial functional tests were performed during the construction process to verify that each component was correctly integrated.

Once the assembly was completed, the prototype parameters were calibrated and adjusted. Extensive testing was performed to determine the optimal axis travel speed, micro wire feed speed, and proper configuration of the electronic components. Fine adjustments were made to optimize the performance and accuracy of the prototype.

Rigorous tests were carried out to evaluate the performance of the prototype. Test welds were performed on different materials and the quality of the joints was analyzed. The execution times were measured and the results obtained were evaluated in comparison with the established standards.

The results obtained during the tests were analyzed and compared with the established objectives and requirements. The strengths and weaknesses of the prototype were identified, as well as possible areas for improvement. The results were documented and decisions were made based on the analysis performed.

Within the framework of this research project, significant results were obtained that contribute to the development and operation of the designed prototype. Correct axis displacement was achieved, proper operation of the micro wire welding machine was obtained, and most of the electronics performed satisfactorily. Although challenges and complications arose, it is recognized the importance of addressing the identified difficulties to optimize the prototype and ensure its optimal performance in future applications and related projects.

Funding

The integrative project has been possible thanks to the valuable financial contribution of the student body. Each student has contributed personal funds and has sought external financing through crowdfunding campaigns and sponsorships. Their financial commitment and efficient resource management has been key to the successful development of the project and the creation of the prototype. Her dedication reflects her passion and belief in this initiative.

Conclusions

In conclusion, the projects developed have represented an important step in the implementation of CNC micro wire welding prototypes. Throughout the process, satisfactory results were obtained in terms of the operation and performance of the prototypes, demonstrating their viability and potential to improve welding processes in the industry.

Each member of the work team had the opportunity to face and learn from different challenges. Areas for improvement were identified in the design, programming and configuration of the electronic components used in the prototypes. These challenges provided valuable experience in problem solving and optimization of the implemented systems.

Although the prototypes showed a performance in line with initial expectations, it is important to highlight that there are still aspects that need to be improved. The need to improve the precise calibration of the displacement axes was identified, especially in the case of the z-axis, where some vibrations were present during the movement. In addition, the importance of having a more effective clamping system to avoid errors in the execution of the welds was recognized.

The recommendations arising from the experience gained are of great relevance for the future development of the prototypes. It is suggested to carry out a more exhaustive research regarding the components used, in order to have a better knowledge of their operation and to be able to face possible challenges more effectively. It is also recommended to implement a periodic maintenance program to guarantee the optimal performance of the control elements and minimize the risk of failures.

In addition, the importance of acquiring a better command of the specific programming language for CNC controllers, such as the G language, is emphasized in order to maximize the capabilities and precision of the prototypes. This will allow taking full advantage of the functionalities of the software used, in this case, the MACH-3 program.

Regarding safety, it is recommended to implement an additional protection system for the operator, since at the current stage the prototypes are in the open. It is essential to ensure the integrity and health of the personnel involved in the operation of the machines.

In summary, the CNC welding projects with micro wire represent a significant advance in the field of automation and improvement of welding processes. The results obtained demonstrate the feasibility and potential of these prototypes to optimize productivity and quality in the joining of metal parts. However, it is necessary to continue working on calibration, research, technical knowledge and the development of support and maintenance systems to achieve optimal performance and greater efficiency in the automated welding process.

Referencias

- Argentina, S. (Julio de 2008). PEU. Obtenido de <https://www.peu.net/syil/mach3.pdf>
- Hernandez, J. (s.f.). Solda Express. Obtenido de <https://soldaexpress.mx/soldadura-por-microalambre-mig-mag-que-es-como-funciona-y-cuales-son-sus-ventajas/#:~:text=Hay%20varios%20tipos%20de%20soldadura,utilizar%20la%20misma%20maquina%20para%20Linuxcnc.> (s.f.). Linuxcnc. Obtenido de https://linuxcnc.org/docs/2.8/html/gcode/overview_es.html#cha:g-code-overview
- Marketing, E. e. (25 de Septiembre de 2019). Tecnologías en soldadura. Obtenido de <https://tecnologiasensoldadura.com.mx/que-es-la-soldadura-por-microalambre/>
- Pacheco, J. (Diciembre de 2014). Repository. Obtenido de https://repository.unilibre.edu.co/bitstream/handle/10901/9843/MONOGRAFIA%20METAL%20CORED_FLUX%20CORED.pdf?sequence=1

Vurcon (s.f.) Vurcon Obtenido de <https://www.vurcon.com/es/en-que-consiste-el-control-numeric-computarizado/>

Urrutia, F. R. (2019, 11 junio). Repositorio Académico Universidad de Chile. <https://repositorio.uchile.cl/handle/2250/169858>

Aguirre, V. F. V. (2019, 8 agosto). Repositorio Digital Universidad Técnica del Norte: Máquina CNC para la elaboración de placas electrónicas; proceso de soldadura y colocación de componentes electrónicos. <http://repositorio.utn.edu.ec/handle/123456789/9387>

Martínez, L. A. M. (2019, 30 octubre). Programación de máquina de soldadura CNC con almacenamiento de datos y visualización en el servidor. <https://upcommons.upc.edu/handle/2117/182269>

Instructions for Scientific, Technological and Innovation Publications

[Title in Times New Roman and Bold No. 14 in English and Spanish]

Surname (IN UPPERCASE), Name 1st Author†*, Surname (IN UPPERCASE), Name 1st Coauthor, Surname (IN UPPERCASE), Name 2nd Coauthor and Surname (IN UPPERCASE), Name 3rd Coauthor

Institutional Affiliation of Author including Dependency (No.10 Times New Roman and Italic)

International Identification of Science - Technology and Innovation

ID 1st Author: (ORC ID - Researcher ID Thomson, arXiv Author ID - PubMed Author ID - Open ID) and CVU 1st author: (Scholar-PNPC or SNI-CONAHCYT) (No.10 Times New Roman)

ID 1st Coauthor: (ORC ID - Researcher ID Thomson, arXiv Author ID - PubMed Author ID - Open ID) and CVU 1st coauthor: (Scholar or SNI) (No.10 Times New Roman)

ID 2nd Coauthor: (ORC ID - Researcher ID Thomson, arXiv Author ID - PubMed Author ID - Open ID) and CVU 2nd coauthor: (Scholar or SNI) (No.10 Times New Roman)

ID 3rd Coauthor: (ORC ID - Researcher ID Thomson, arXiv Author ID - PubMed Author ID - Open ID) and CVU 3rd coauthor: (Scholar or SNI) (No.10 Times New Roman)

(Report Submission Date: Month, Day, and Year); Accepted (Insert date of Acceptance: Use Only ECORFAN)

Abstract (In English, 150-200 words)

Objectives
Methodology
Contribution

Keywords (In English)

Indicate 3 keywords in Times New Roman and Bold No. 10

Abstract (In Spanish, 150-200 words)

Objectives
Methodology
Contribution

Keywords (In Spanish)

Indicate 3 keywords in Times New Roman and Bold No. 10

(Citation: Surname (IN UPPERCASE), Name 1st Author, Surname (IN UPPERCASE), Name 1st Coauthor, Surname (IN UPPERCASE), Name 2nd Coauthor and Surname IN UPPERCASE), Name 3rd Coauthor. Paper Title. Journal of Technological Operations. Year 1-1: 1-11 [Times New Roman No.10]

* Author Correspondence (ejemplo@ejemplo.org).

† Researcher contributing as first author.

Instructions for Scientific, Technological and Innovation Publications

Introduction

Text in Times New Roman No.12, single space.

General explanation of the subject and explain why it is important.

What is your added value with respect to other techniques?

Clearly focus each of its features

Clearly explain the problem to be solved and the central hypothesis.

Explanation of sections Article.

Development of headings and subheadings of the article with subsequent numbers

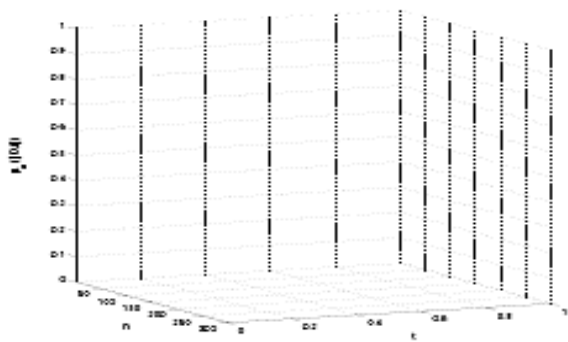
[Title No.12 in Times New Roman, single spaced and bold]

Products in development No.12 Times New Roman, single spaced.

Including graphs, figures and tables-Editable

In the article content any graphic, table and figure should be editable formats that can change size, type and number of letter, for the purposes of edition, these must be high quality, not pixelated and should be noticeable even reducing image scale.

[Indicating the title at the bottom with No.10 and Times New Roman Bold]



Graphic 1 Title and *Source (in italics)*

Should not be images-everything must be editable.

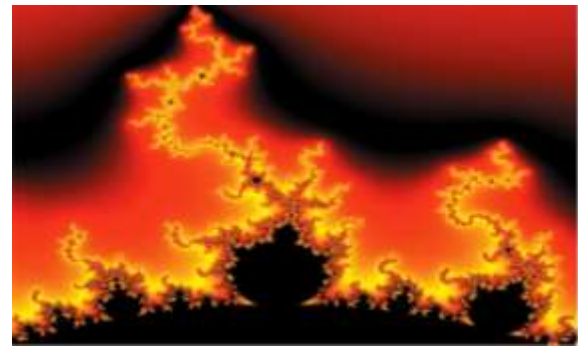


Figure 1 Title and *Source (in italics)*

Should not be images-everything must be editable.

Table 1 Title and *Source (in italics)*

Should not be images-everything must be editable.

Each article shall present separately in **3 folders**: a) Figures, b) Charts and c) Tables in .JPG format, indicating the number and sequential Bold Title.

For the use of equations, noted as follows:

$$Y_{ij} = \alpha + \sum_{h=1}^r \beta_h X_{hij} + u_j + e_{ij} \quad (1)$$

Must be editable and number aligned on the right side.

Methodology

Develop give the meaning of the variables in linear writing and important is the comparison of the used criteria.

Results

The results shall be by section of the article.

Annexes

Tables and adequate sources

Thanks

Indicate if they were financed by any institution, University or company.

Conclusions

Explain clearly the results and possibilities of improvement.

References

Use APA system. Should not be numbered, nor with bullets, however if necessary numbering will be because reference or mention is made somewhere in the Article.

Use Roman Alphabet, all references you have used must be in the Roman Alphabet, even if you have quoted an Article, book in any of the official languages of the United Nations (English, French, German, Chinese, Russian, Portuguese, Italian, Spanish, Arabic), you must write the reference in Roman script and not in any of the official languages.

Technical Specifications

Each article must submit your dates into a Word document (.docx):

Journal Name

Article title

Abstract

Keywords

Article sections, for example:

1. *Introduction*
2. *Description of the method*
3. *Analysis from the regression demand curve*
4. *Results*
5. *Thanks*
6. *Conclusions*
7. *References*

Author Name (s)

Email Correspondence to Author

References

Intellectual Property Requirements for editing:

- Authentic Signature in Color of Originality Format Author and Coauthors
- Authentic Signature in Color of the Acceptance Format of Author and Coauthors
- Authentic Signature in Color of the Conflict of Interest Format of Author and Co-authors.

Reservation to Editorial Policy

Journal of Technological Operations reserves the right to make editorial changes required to adapt the Articles to the Editorial Policy of the Research Journal. Once the Article is accepted in its final version, the Research Journal will send the author the proofs for review. ECORFAN® will only accept the correction of errata and errors or omissions arising from the editing process of the Research Journal, reserving in full the copyrights and content dissemination. No deletions, substitutions or additions that alter the formation of the Article will be accepted.

Code of Ethics - Good Practices and Declaration of Solution to Editorial Conflicts

Declaration of Originality and unpublished character of the Article, of Authors, on the obtaining of data and interpretation of results, Acknowledgments, Conflict of interests, Assignment of rights and Distribution.

The ECORFAN-Mexico, S.C Management claims to Authors of Articles that its content must be original, unpublished and of Scientific, Technological and Innovation content to be submitted for evaluation.

The Authors signing the Article must be the same that have contributed to its conception, realization and development, as well as obtaining the data, interpreting the results, drafting and reviewing it. The Corresponding Author of the proposed Article will request the form that follows.

Article title:

- The sending of an Article to Journal of Technological Operations emanates the commitment of the author not to submit it simultaneously to the consideration of other series publications for it must complement the Format of Originality for its Article, unless it is rejected by the Arbitration Committee, it may be withdrawn.
- None of the data presented in this article has been plagiarized or invented. The original data are clearly distinguished from those already published. And it is known of the test in PLAGSCAN if a level of plagiarism is detected Positive will not proceed to arbitrate.
- References are cited on which the information contained in the Article is based, as well as theories and data from other previously published Articles.
- The authors sign the Format of Authorization for their Article to be disseminated by means that ECORFAN-Mexico, S.C. In its Holding Taiwan considers pertinent for disclosure and diffusion of its Article its Rights of Work.
- Consent has been obtained from those who have contributed unpublished data obtained through verbal or written communication, and such communication and Authorship are adequately identified.
- The Author and Co-Authors who sign this work have participated in its planning, design and execution, as well as in the interpretation of the results. They also critically reviewed the paper, approved its final version and agreed with its publication.
- No signature responsible for the work has been omitted and the criteria of Scientific Authorization are satisfied.
- The results of this Article have been interpreted objectively. Any results contrary to the point of view of those who sign are exposed and discussed in the Article.

Copyright and Access

The publication of this Article supposes the transfer of the copyright to ECORFAN-Mexico, SC in its Holding Taiwan for its Journal of Technological Operations, which reserves the right to distribute on the Web the published version of the Article and the making available of the Article in This format supposes for its Authors the fulfilment of what is established in the Law of Science and Technology of the United Mexican States, regarding the obligation to allow access to the results of Scientific Research.

Article Title:

Name and Surnames of the Contact Author and the Coauthors	Signature
1.	
2.	
3.	
4.	

Principles of Ethics and Declaration of Solution to Editorial Conflicts

Editor Responsibilities

The Publisher undertakes to guarantee the confidentiality of the evaluation process, it may not disclose to the Arbitrators the identity of the Authors, nor may it reveal the identity of the Arbitrators at any time.

The Editor assumes the responsibility to properly inform the Author of the stage of the editorial process in which the text is sent, as well as the resolutions of Double-Blind Review.

The Editor should evaluate manuscripts and their intellectual content without distinction of race, gender, sexual orientation, religious beliefs, ethnicity, nationality, or the political philosophy of the Authors.

The Editor and his editing team of ECORFAN® Holdings will not disclose any information about Articles submitted to anyone other than the corresponding Author.

The Editor should make fair and impartial decisions and ensure a fair Double-Blind Review.

Responsibilities of the Editorial Board

The description of the peer review processes is made known by the Editorial Board in order that the Authors know what the evaluation criteria are and will always be willing to justify any controversy in the evaluation process. In case of Plagiarism Detection to the Article the Committee notifies the Authors for Violation to the Right of Scientific, Technological and Innovation Authorization.

Responsibilities of the Arbitration Committee

The Arbitrators undertake to notify about any unethical conduct by the Authors and to indicate all the information that may be reason to reject the publication of the Articles. In addition, they must undertake to keep confidential information related to the Articles they evaluate.

Any manuscript received for your arbitration must be treated as confidential, should not be displayed or discussed with other experts, except with the permission of the Editor.

The Arbitrators must be conducted objectively, any personal criticism of the Author is inappropriate.

The Arbitrators must express their points of view with clarity and with valid arguments that contribute to the Scientific, Technological and Innovation of the Author.

The Arbitrators should not evaluate manuscripts in which they have conflicts of interest and have been notified to the Editor before submitting the Article for Double-Blind Review.

Responsibilities of the Authors

Authors must guarantee that their articles are the product of their original work and that the data has been obtained ethically.

Authors must ensure that they have not been previously published or that they are not considered in another serial publication.

Authors must strictly follow the rules for the publication of Defined Articles by the Editorial Board.

The authors have requested that the text in all its forms be an unethical editorial behavior and is unacceptable, consequently, any manuscript that incurs in plagiarism is eliminated and not considered for publication.

Authors should cite publications that have been influential in the nature of the Article submitted to arbitration.

Information services

Indexation - Bases and Repositories

RESEARCH GATE (Germany)

GOOGLE SCHOLAR (Citation indices-Google)

MENDELEY (Bibliographic References Manager)

REDIB (Ibero-American Network of Innovation and Scientific Knowledge- CSIC)

HISPANA (Information and Bibliographic Orientation-Spain)

Publishing Services

Citation and Index Identification H

Management of Originality Format and Authorization

Testing Article with PLAGSCAN

Article Evaluation

Certificate of Double-Blind Review

Article Edition

Web layout

Indexing and Repository

Article Translation

Article Publication

Certificate of Article

Service Billing

Editorial Policy and Management

69 Street. YongHe district, ZhongXin. Taipei-Taiwan. Phones: +52 1 55 6159 2296, +52 1 55 1260 0355, +52 1 55 6034 9181; Email: contact@ecorfan.org www.ecorfan.org

ECORFAN®

Chief Editor

BARRERO-ROSALES, José Luis. PhD

Executive Director

RAMOS-ESCAMILLA, María. PhD

Editorial Director

PERALTA-CASTRO, Enrique. MsC

Web Designer

ESCAMILLA-BOUCHAN, Imelda. PhD

Web Diagrammer

LUNA-SOTO, Vladimir. PhD

Editorial Assistant

SORIANO-VELASCO, Jesús. BsC

Philologist

RAMOS-ARANCIBIA, Alejandra. BsC

Advertising & Sponsorship

(ECORFAN® Taiwan), sponsorships@ecorfan.org

Site Licences

03-2010-032610094200-01-For printed material ,03-2010-031613323600-01-For Electronic material,03-2010-032610105200-01-For Photographic material,03-2010-032610115700-14-For the facts Compilation,04-2010-031613323600-01-For its Web page,19502-For the Iberoamerican and Caribbean Indexation,20-281 HB9-For its indexation in Latin-American in Social Sciences and Humanities,671-For its indexing in Electronic Scientific Journals Spanish and Latin-America,7045008-For its divulgation and edition in the Ministry of Education and Culture-Spain,25409-For its repository in the Biblioteca Universitaria-Madrid,16258-For its indexing in the Dialnet,20589-For its indexing in the edited Journals in the countries of Iberian-America and the Caribbean, 15048-For the international registration of Congress and Colloquiums. financingprograms@ecorfan.org

Management Offices

69 Street. YongHe district, ZhongXin. Taipei-Taiwan.

Journal of Technological Operations

"Precision analysis of the integration rules used for transient simulation in electric networks"

GALVÁN-SÁNCHEZ, Verónica Adriana, BAÑUELOS-CABRAL, Eduardo Salvador, GARCÍA-SÁNCHEZ, Jorge Luis and SOTELO-CASTAÑÓN, Julián

Universidad de Guadalajara

"Maintenance management of pneumatic equipment and facilities at a plant in the Industrial corridor in the South area of the state of Tamaulipas"

CRUZ-SUSTAITA, Vianey, LERMA-LEDEZMA, David and ESPINOSA-SOSA, Enrique Esteban

Universidad Politécnica de Altamira

"Simulation of the behavior of the flow of electrons between the electrodes of a thermionic converter"

CALVARIO-GONZÁLEZ, Abdías, BARBOSA-SANTILLÁN, Luis Francisco and JUÁREZ-VARELA, Mirna Patricia

Universidad Tecnológica de Puebla

"Integrative project: CNC technology and micro-wire (MIG) welding for precision and efficiency in industry"

ZUNIGA-MORENO, Juan, COTERO-RODRÍGUEZ, Arely Eunice and MORALES HERNÁNDEZ, Victor

Universidad Tecnológica Cadereyta

